





Article

Trends and Extremes of Drought Episodes in Vietnam Sub-Regions during 1980–2017 at Different Timescales

Milica Stojanovic ¹, Margarida L.R. Liberato ^{1,2,*} , Rogert Sorí ^{1,3}, Marta Vázquez ^{1,2,3} ,
Tan Phan-Van ⁴, Hieu Duongvan ⁵, Tin Hoang Cong ⁵ , Phuong N. B. Nguyen ⁴, Raquel Nieto ³ 
and Luis Gimeno ³

¹ Instituto Dom Luiz, Faculdade de Ciências da Universidade de Lisboa, 1749-016 Campo Grande, Portugal; mstojanovic@fc.ul.pt (M.S.); roger.sori@uvigo.es (R.S.); martavazquez@uvigo.es (M.V.)

² Escola de Ciências e Tecnologia, Universidade de Trás-os-Montes e Alto Douro, 5001-801 Vila Real, Portugal

³ Environmental Physics Laboratory (EPhysLab), CIM-Uvigo, Universidade de Vigo, 32004 Ourense, Spain; rnieto@uvigo.es (R.N.); l.gimeno@uvigo.es (L.G.)

⁴ Department of Meteorology and Climate Change, VNU University of Science, 334 Nguyen Trai, Thanh Xuan, Hanoi 100000, Vietnam; tanpv@vnu.edu.vn (T.P.-V.); phuongnbn@hus.edu.vn (P.N.B.N.)

⁵ Department of Environmental Science, University of Sciences-Hue University, 77 Nguyen Hue Street, Hue 530000, Vietnam; dvhieu@hueuni.edu.vn (H.D.); hoangcongtn@hueuni.edu.vn (T.H.C.)

* Correspondence: mlr@utad.pt

Received: 31 December 2019; Accepted: 10 March 2020; Published: 14 March 2020



Abstract: This study investigated the temporal occurrence of dry conditions in the seven climatic sub-regions of Vietnam during the 1980–2017 period. This assessment was performed using the Standardized Precipitation Evapotranspiration Index (SPEI) and the Standardized Precipitation Index (SPI) at 1 to 24 months timescales. Results show that the main periods of extreme drought occurred simultaneously throughout the country in 1992–1993 and 2003–2004, except for 2015–2016, when it was not identified in the southern region. In addition, a slight temporal lag was identified latitudinally (north–south) at the beginning of dry conditions, revealing the largest difference between the northern and southern regions. A positive trend in the time series of both indices (SPEI and SPI) prevailed in all sub-regions, with the SPEI minus SPI difference always being negative, suggesting the importance of temperature and evapotranspiration for this trend. Further detailed analyses were then performed using SPEI at 1-month and 12-months timescales for all climate sub-regions, as well as the main indicators to characterize duration and severity. Results show that the number of drought episodes did not vary much between regions, but they did vary in duration and severity at the annual scale. Moreover, changes in the soil root zone are largely associated with dry and wet conditions not only from season to season, but also in longer accumulation periods and more strongly in the northern regions of Vietnam. Indeed, a study of the most severe drought episodes also revealed the occurrence of negative anomalies of the root-soil moisture in the subsequent four or more months. Dynamic atmospheric conditions associated with the peak of most severe drought episodes show the crucial role of subsidence of dry air in the middle and high atmosphere, which prevents convection in the lower troposphere. Finally, the linkages between drought conditions in Vietnam and large-scale atmospheric and oceanic teleconnection patterns were revealed to be quite different among northern and southern sub-regions. During the positive phase of El Niño–Southern Oscillation (ENSO), drought episodes at different timescales were identified in the southern climate sub-regions, while the negative phase was associated with drought conditions in the northern regions.

Keywords: droughts; Vietnam; SPEI; soil moisture; teleconnection patterns

1. Introduction

Droughts are part of the natural climate system and can be defined as a complex phenomenon that occurs when water availability is significantly less than regular levels for an extended period and the available water cannot satisfy the demand [1–4]. The temporal and spatial variability of droughts as well as the large number of systems that it can affect make this phenomenon difficult to quantify. Therefore, there is no universal definition of drought [5–8]. Its onset, duration, end, and severity are not easily measurable [9–11], and their effects can slowly accumulate over a substantial period of time, affecting large geographical areas [3,12,13] and numerous sectors, such as environment, agriculture, economy, and society. Hence, droughts are usually classified into four major categories: meteorological, agricultural, hydrological, and socioeconomic droughts [2,14,15]. Meteorological droughts are defined as below-average amounts of precipitation for a certain period of time, and may be combined with increased potential evapotranspiration (PET) [16–18]. Through land-atmosphere interactions, prolonged meteorological drought can further exacerbate agricultural drought, or even hydrological drought [12,19–21]. Therefore, efficient monitoring of meteorological droughts is necessary in order to provide early warnings and perform risk management in regions with limited water resources or high agricultural production dependent on irrigation.

Some studies have highlighted that droughts have become unusually more frequent and severe worldwide, such as in the Mediterranean region [21–23], Europe [24–26], West Africa [27,28], and Asia, including Vietnam [20,29–35]. Recent conclusions of the Intergovernmental Panel on Climate Change (IPCC) show much evidence that climate change affects many regions in Southeast Asia, one of the most vulnerable regions in the world [36,37]. Vietnam is likely to be one of the countries most affected by climate change because of its long coastline and strong reliance on agriculture, natural resources, and forestry [34,38–41]. Few publications have investigated the characteristics of droughts in this region (e.g., [32,35,42–45]). Tue and co-authors [32] investigated drought over the Central Highland using the Standardized Precipitation Index (SPI) with different observed and modeled monthly precipitation datasets for the period 1990–2005. Their results showed that regional climate models data successfully captured the spatial structure of the SPI; in particular, the severe drought events of 1998 and 2005. For a longer study period, Le et al. [35] studied the spatio-temporal variability of drought in Vietnam for the period 1980–2014, but using the Palmer Drought Severity Index (PDSI). Their results showed regional patterns of drought duration, frequency, and severity, but no consistent trend of drought during the study period. Although the country is narrow, spatial differences of meteorological drought severity for South Central and the Central Highlands are documented [42]. In the north of the country, the Cai River Basin has also experienced relatively high drought severity in the period of 1982 to 2012 [43], while extreme drought affected the Ba River basin in South-Central Vietnam during 2013 and 2016 [44]. Other authors, such as Vu-Thanh et al. [45], investigated the occurrence of drought through several drought indices for the period 1961–2007, considering Vietnam divided into seven sub-regions. Their results revealed that in the southern sub-regions of Vietnam drought mainly occurred during El Niño years, while wet conditions were frequently observed in the La Niña years.

Drought predictability is a current challenge for hydrometeorological sciences and it has also been assessed for some regions of Vietnam, such as the Khanhhoa Province Vietnam [46] or South-Central Vietnam [47]. Statistical techniques have also been used to evaluate the influence of different infilling techniques on the spatial distribution of the Standardized Precipitation Evapotranspiration Index (SPEI) in the South-Central Region of Vietnam [48]. In terms of drought impacts, these have been quantified for well-known dry periods, such as the extremely strong drought event in 1982–1983, which had severe impacts on the environmental and socio-economic sectors of Vietnam [49]. Another example is the 1997–1998 drought, when the total losses in terms of agricultural production were about 400 million US dollars [44,50]. Furthermore, the drought episode that occurred in 2003 caused the main impacts on the coffee sector of Vietnam, thereby emphasizing the role of the detection of drought as an important issue [29]. As a result of the 2015–2016 drought, the discharges of the main rivers decreased by 20–90% and crop damage was serious, with 60–90% of planted crops being damaged in drought-affected

areas [51]. Although it is still impossible to avoid droughts, an effective and timely monitoring system in Vietnam is required so that they can be predicted and their effects can be lessened.

During the 1958–2007 period, the annual mean temperature of the Vietnam area increased by around 0.5–0.7 °C [34,52]. According to Nguyen et al. [53], in all sub-regions, it increased at a rate of 0.26 ± 0.10 °C in the period 1971–2010, and this rate was greater in winter than in summer. Annual mean temperatures in southern regions are rising quicker than in the northern ones. The concern arises if we also consider that besides the precipitation, high temperatures also modulate the occurrence of droughts [35]. An impact assessment based on climate change scenarios (precipitation and temperature) for the Lower Mekong River Basin for the period of 2016–2040 [54] indicates an increase in temperature and a decrease in precipitation in the near future, significantly decreasing the streamflow and soil water content, while drought characteristics in terms of severity, duration, and frequency are projected to be increased.

Therefore, more hydrometeorological research is necessary as far as Vietnam is concerned; not only in understanding climate and its changes, but also to be able to comprehend extreme events such as droughts and their severity. This may contribute to increasing the hydroclimate knowledge of Vietnam as well as to support early drought warning in order to develop effective mitigation strategies. Therefore, the objectives of this study are: (i) to investigate the occurrence of dry conditions that affected the seven main climatological sub-regions of Vietnam during recent decades (1980–2017) using the SPI and the Standardized Precipitation Evapotranspiration Index (SPEI) at several timescales and computed for Climate Research Unit (CRU) Time-Series (TS) v.4.02 gridded datasets; (ii) to identify the occurrence of drought episodes, their characteristics and propagation through the root soil moisture; and as a third aim (iii) to explore driving mechanisms of the most severe meteorological episode for each of the seven sub-regions of Vietnam. Specifically, to explore the role of teleconnection patterns on the occurrence of dry conditions, particularly the role of ENSO.

Despite previous research on droughts in Vietnam, referenced above, the novelty of our study is mainly related to the assessment of the most extreme drought events. We expect that our results may contribute to increasing the hydroclimate knowledge of the region and support early drought warning, agricultural, and forest management plans in order to develop effective mitigation strategies for Vietnam.

Study Area

Vietnam is situated in Southeast Asia on the eastern part of the Indochina Peninsula, in the centre of two main tropical monsoon areas, the South Asian (southwest) and the East Asian (northeast) monsoons among the latitudes 7.5° N and 22.5° N and longitudes of 102° E and 109° E. The area of Vietnam is small (around 330,000 km²) and three-quarters of its territory is covered by mountains and hills, with the highest peaks 3000 m tall. From North to South there are nine major river systems, counting the Mekong River in the South and Red River in the North. Besides the South China Sea, two large gulfs, the Tonkin gulf (situated in the North) and the Thailand gulf (situated in the South) are a significant part of Vietnam's hydrological resources [53]. The climate of the country is very diverse and is strongly influenced by monsoon circulation and the topography [32,53,55,56]. Vietnam's climate is mostly affected by Asian monsoon systems: the southwest monsoon in the summer season and the northeast monsoon in the winter season. The southwest Asian summer monsoon and the northeast Asian winter monsoon are related to a wet and a dry season, respectively. The wet season occurs from May to October, whereas the dry season is from November to April [57]. During summer time, the southwest monsoon brings moisture in the air from the Bay of Bengal to the country, initiating the rainy season in the south and central highland sub-regions. This time is also the rainy season in the northern parts of country, but rainfall originates mainly from the activity of the Intertropical Convergence Zone (ITCZ), tropical cyclones, and part of the southwest monsoon.

The northern part of Vietnam has a tropical monsoon climate influenced by the northeast monsoon, which produces cold, dry climate conditions in early winter, while in late winter, it produces cold, highly humid conditions. Although the winter monsoon is primarily dry, due to it coming from the

Asian continent, the clash with the mild and humid air of the Gulf of Tonkin creates frequent rains. In this period the dry season also occurs in the south and central highland, but the difference is that in the northern parts the number of rainy days is much more than in the southern parts of the country. Southern Vietnam has quite a moderate tropical climate (due to the impacts of the southwest monsoon) and is characterized by dry and rainy seasons [55,56]. The rainy season in the north central and south central sub-regions starts in about mid-August and ends in about mid-December, while the dry season is from January to July. In the summer, the temperature is very high, with the peak often happening in June, while the highest precipitation rates are in May and August [58]. The mean annual precipitation over the country is around 1400–2400 mm and can differ from 700 up to 5000 mm, depending on the sub-region [32,59]. Regarding its complex topography and differences in precipitation and temperature conditions, it is categorized into seven climate sub-regions: the North West (S1), North East (S2), North Plain (Red River Delta) (S3), North Central (S4), South Central (S5), Central Highland (S6), and the South (S7) regions, shown in Figure 1 [41,55,58].

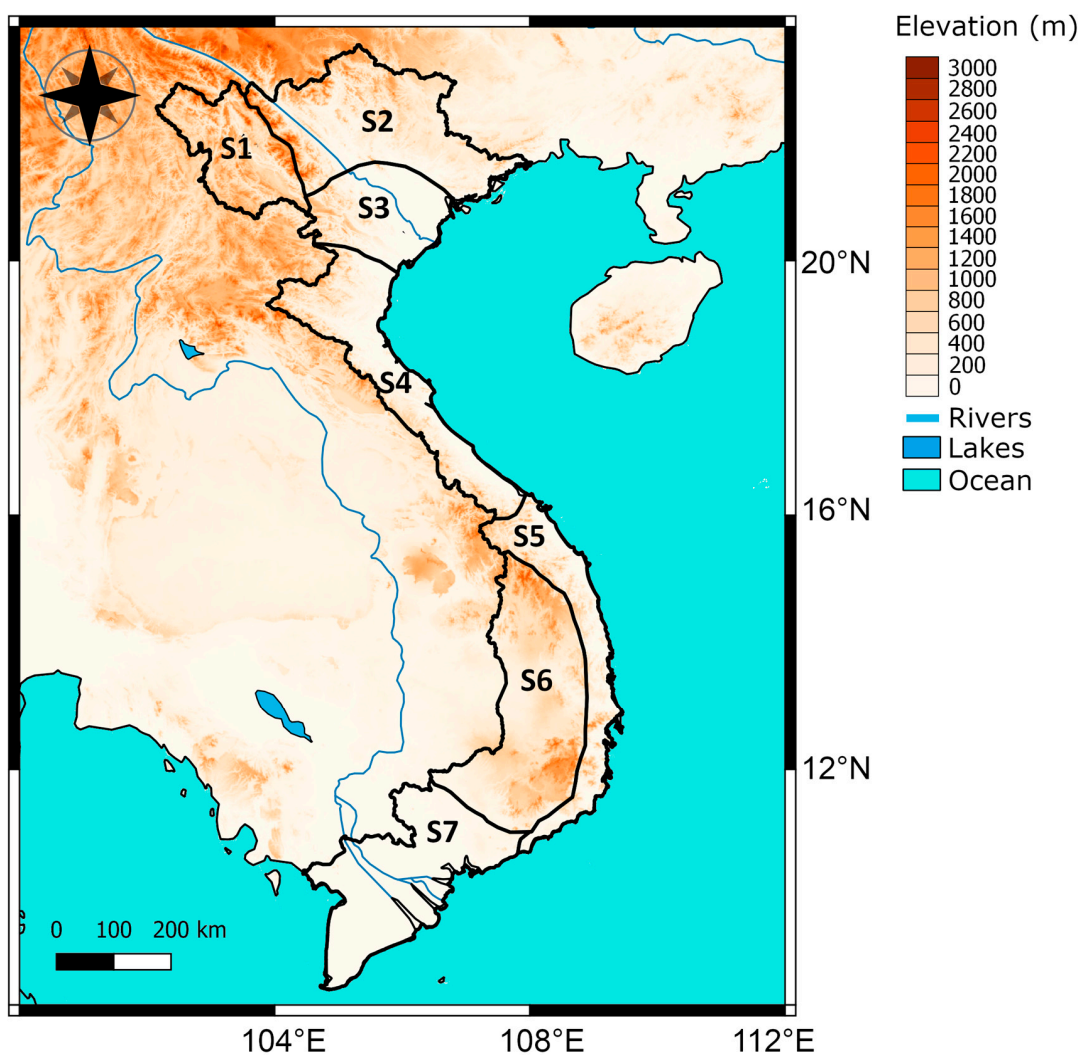


Figure 1. S1–S7 seven climate sub-regions of Vietnam. Colors represent the elevation of the region in meters. Data obtained from the HydroSHEDS project (hydrological data and maps on shuttle elevation derivatives at multiple scales available online at <https://hydrosheds.cr.usgs.gov/>).

2. Data and Methodology

2.1. Drought Identification

Diverse indices have been developed and used for identifying and monitoring droughts [60]. In particular, a great number of studies identifying and investigating the causes and impacts of droughts have employed the Palmer Drought Severity Index (PDSI) [61,62] and the Standardized Precipitation Index (SPI) [63], based on the soil-water balance equation and a precipitation probabilistic approach, respectively. The Standardized Precipitation Evapotranspiration Index (SPEI) [64,65], based on the procedure originally used to compute the SPI, was created to overcome the deficiencies of the PDSI and the SPI, and is based on a climatic water balance (PRE (precipitation) minus PET (potential evapotranspiration)) that may be computed at different timescales. The PET values in this study were obtained from the Climate Research Unit (CRU) Time-Series (TS) v4.02. To obtain PET values, a modified version of the Penman–Monteith Reference Evapotranspiration (ET_o) equation was used in the CRU dataset as a metric of the PET. This ET_o can be associated with the PET, since resistance factors are not temporally and spatially variable and only depend on the four main meteorological drivers of PET (air temperature, radiation, atmospheric humidity, and wind speed, as is the case for FAO-56 crop reference evaporation) [66]. The timescales are connected to different types of drought, with the short timescales (e.g., 1 month) representing meteorological drought, and the longest timescales of 12, 18, and 24 months representing drought in hydrological systems under natural flow conditions. Therefore, it combines the sensitivity of the PDSI to the changes in evapotranspiration demand with the multi-temporal nature of the SPI [17,67–69]. A detailed description of SPI is not stated here, please refer to [61] for more information.

To calculate the SPEI, a log-logistic probability distribution is used to transform the calculated (PRE–PET) values to standardized units, in which dry conditions are represented by negative values and wet conditions are represented by positive values. Other probability distributions could be applied, but the SPEI designers recommended the log-logistic probability distribution because it offers better SPEI time series results than other distributions [64]. The SPEI is computed in temporal frequencies from 1 to 24 months by considering the climatic water balance of the previous months.

A crucial advantage of the SPEI over other widely used indices is that it combines multiscalar characteristics and temperature data in the analysis of drought. This makes SPEI likely to be more appropriate to use under global warming conditions if we consider that (i) higher temperatures have been found to affect the severity of droughts [3,64,70–73] and also (ii) the multiscalar character allows the evaluation of drought conditions, considering different timescales. Therefore, the Standardized Precipitation Evapotranspiration Index (SPEI) was used to determine the evolution of dry conditions at each of the Vietnam climate sub-regions during the period 1980–2017.

For the identification of meteorological and long-term drought episodes, all the timescales from 1 to 24 months SPEI were used. A detailed analysis was performed for the 1, 12, 18, and 24 months (SPEI01, SPEI12, SPEI18, and SPEI24, respectively). The SPEI01 mostly represents the water balance for one month and it is commonly used to identify the occurrence of meteorological droughts [74].

After the calculation of the index, a trend analysis based on simple linear regression analysis was performed and statistical significance was considered at 95% confidence level (p -value < 0.05 computed using the Wald Test with t -distribution [75]). The Wald test (W) is a statistical test commonly used to verify the null hypothesis in linear regression analysis based on the maximum likelihood estimation (MLE). The test for a single parameter, considering 0 the null hypothesis, follows the formulation:

$$W = \frac{\hat{\beta}}{\sigma}, \quad (1)$$

where $\hat{\beta}$ is the MLE estimator and σ its standard deviation.

According to Agnew [76], the drought episodes can be classified into three categories (moderately dry, severely dry, and extremely dry; Table 1). This categorization is based on the probability classes to identify the severity of each dry period rather than the magnitudes of the SPI, and because of that, it is proposed as a more reasonable approach. The same categories can be used for SPEI because SPEI computation is based on the original SPI calculation procedure. The main difference with the SPI is that calculation is exclusively based on precipitation, while the SPEI uses the difference between precipitation and PET. Drought differs from other natural disasters in many ways and it is particularly difficult to define when a drought starts and when it is over [9–11]. A drought episode onset is defined when the SPEI falls below -0.84 and it ends when the SPEI returns to a positive value. When a drought episode is identified, the peak value, duration, and severity may be calculated. The peak value of a drought episode is the largest negative magnitude recorded during the episode. Duration indicates the number of months between the first and last months of the episode, and the severity is calculated as the sum of all SPEI values (absolute values) during the episode.

Table 1. Standardized Precipitation Evapotranspiration Index (SPEI) classification according to the Standardized Precipitation Index (SPI) classification proposed by Agnew [76].

SPEI	Probability	Category
>1.65	0.05	Extremely humid
>1.28	0.1	Severely humid
>0.84	0.2	Moderately humid
>-0.84 and <0.84	0.6	Normal
<-0.84	0.2	Moderately dry
<-1.28	0.1	Severely dry
<-1.65	0.05	Extremely dry

2.2. Data

The SPEI was computed using the PRE and PET datasets from the Climate Research Unit (CRU) Time-Series (TS) v4.02 at a spatial resolution of 0.5° in longitude and latitude [77]. The SPI was computed using the PRE from the same source. The mean temperature from this dataset was also used. Soil moisture root (SMroot) data belonged to the Global Land Model (GLEAM) v3.0 [78,79]. The period of study was 1980–2017.

Monthly gridded data of omega (dq/dt), air temperature (T), and relative humidity (RH) from the NCEP-DOE AMIP-II Reanalysis (R-2) [80] provided by the National Oceanic and Atmospheric Administration (NOAA) Earth System Research Laboratory's (ESRL) Physical Sciences Division (PSD) (<https://www.esrl.noaa.gov/psd/>) were used to investigate vertical motions and respective anomalies along 12 pressure levels, from 1000 mb to 100 mb, during the most severe drought episodes for each one of the seven sub-regions of Vietnam. Monthly anomalies were computed as departures of the considered field (for a given month) from the reference long-term (1981–2010) mean climatological field (for that month). Composites of meteorological fields and of respective anomalies for each considered period were finally derived by averaging the fields over the periods. This reanalysis project is an improved version of the NCEP Reanalysis I model that fixed errors and updated parameterizations of physical processes.

The climate modes used in this study were Bivariate El Niño Southern Oscillation time series (BEST), Dipole Mode Index (DMI), Western Hemisphere Warm Pool (WHWP), Southern Oscillation Index (SOI), Pacific Decadal Oscillation (PDO), and East Central Tropical Pacific Sea Surface Temperature (SST) (ENSO 3.4). These datasets were downloaded from NOAA ESRL Physical Sciences Division (PSD) at <https://www.esrl.noaa.gov/psd/data/climateindices/list/>.

3. Results and Discussion

3.1. Climatological Annual Cycle

The hydrological annual cycle of PRE, PET, and mean temperature for the 1980–2017 period for each of the seven sub-regions of Vietnam are represented in Figure 2. As observed, the occurrence of the maximum PRE varied in time according to the latitudinal variation between the northern regions (S1, S2) and the southern ones (S7). In the northern regions (S1, S2, S3), the rainy season extended from May to October, and the rainiest months were July and August (more than 270 mm/month). In the remaining months, from December to February, the minimum average PRE (<25 mm/month) occurred. The PET values in these regions were lower than PRE values, but both followed a similar annual cycle. Average temperatures ranged from 24 to 28 °C in summer to 15 to 20 °C in winter. In the central part of Vietnam, the PRE over the S4 region reflected a transition of the pluviometry of the country. The S4 region, unlike the northern regions, received a greater amount of precipitation in the final months of the year. PET values remained lower than PRE. In the regions S5 and S6 a rapid rise in average precipitation values was observed from September, with a maximum in October (more than 360 mm/month), usually attributed to rainfalls associated with tropical cyclones and typhoons [49]. In both regions, the mean temperature ranged from 21 to 25 °C, with the highest values during May–August, which corresponds with the rapid warming of the landmass that causes the onset of the South Asian summer monsoon with atmospheric circulation over mid and low latitudes [81]. Besides, PET values exceeded PRE from January to April. Southern Vietnam has a quite moderate tropical climate due to the impacts of the southwest monsoon and is characterized by dry and rainy seasons [55,56]. In the southern part of the country (S7), the rainy period covered from May to November, without great differences in average amounts between June to October. The average temperatures ranged from 28 to 29 °C in summer to 26 to 27.5 °C in winter. The average temperature in this region hardly changed during the year, and the PET exceeded the PRE only from January to April.

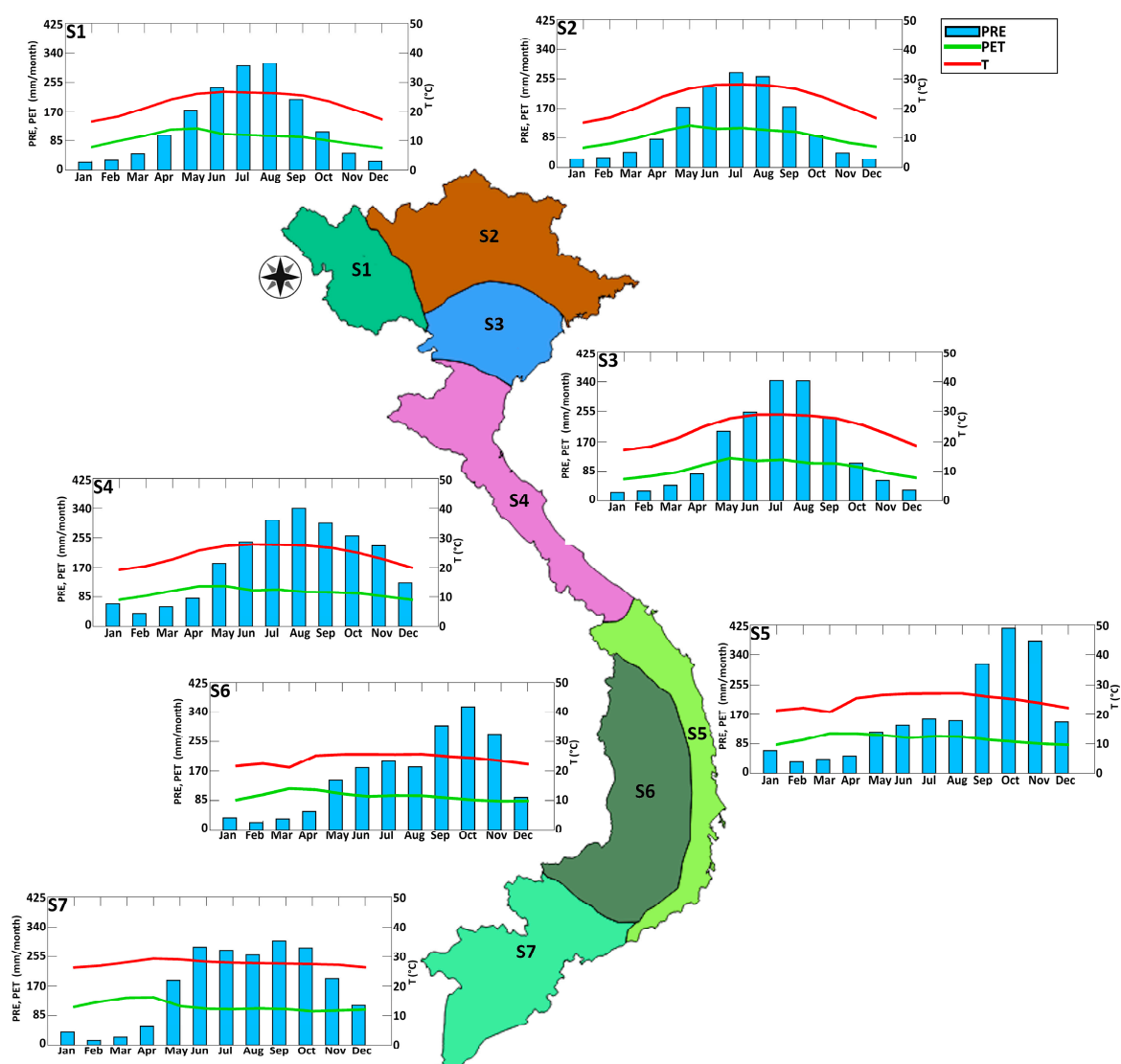


Figure 2. The climatological annual cycle for each of the seven sub-regions of Vietnam in the period 1980–2017. The blue bars represent the annual cycle of precipitation (PRE, mm/month), the green lines represent the potential evapotranspiration (PET, mm/month) and the red lines represent the mean air temperature (T, °C).

3.2. Drought Conditions

Figure 3 shows the temporal evolution of drought conditions for every sub-region of Vietnam according to the SPEI and SPI computed for 1- to 24-months timescales and classified according to those ranges shown in Table 1. For sub-region S1 both the SPEI and SPI were able to represent with great similarity the temporal occurrence of drought conditions in all the timescales, even the extreme droughts occurring in 1992 and at the end of 2009. However, there were some slight differences in relation to the magnitude. This is the case for the drought event that began at the end of 2009 and prolonged through timescales until 2012. It is also perceptible that several drought events did not prolong across the 24-month timescale. For the regions S2 and S3 the beginning of drought and the temporal pattern of different drought categories across the 24-month timescale of the index greatly match those identified for S1. S4 showed major differences in the temporal evolution of drought conditions, in which a temporal displacement of the beginning of the drought conditions occurred around 1992. Besides this, the 2015–2016 period was affected by moderate, severe, and extreme drought conditions. This was also observed in the southernmost regions (S5, S6, and S7). In terms of damage,

the 2015–2016 drought has been documented as being the worst drought in Vietnam in 90 years and it has been attributed to the El Niño weather event [82]. Similar temporal evolution of drought conditions as in S4 was observed in S5 and S6. The SPI in S6 seemed to reproduce less intense drought conditions than SPEI in 1980, 1992–1993, and 2004–2005. Finally, the temporal evolution of different types of droughts in the southern region of the country (S7) illustrated that an intense drought period affected this region at the end of 1982 and the beginning of 1983 and, contrary to the rest of the sub-regions, S7 was not affected by the 2015–2016 dry period.

The drought periods described above are in accordance with the study of Le and colleagues [35], who used monthly precipitation and 2 m air temperature observations for the period 1980–2014 obtained from 131 meteorological stations across mainland Vietnam to calculate PDSI. However, these authors [35] found that in the S5 region the dry conditions were more intense than in the other regions of the country, and this is not clearly noticeable in our results.

To investigate the overall trend of SPEI and SPI values at different timescales (1, 12, 18, 24 months) during the period 1980–2017 for each of the seven sub-regions of Vietnam, the Wald test with t-distribution [75] was applied. Table 2 shows for SPEI01 a positive trend for S1, S4, S5, S6, and S7, and a negative trend for S2 and S3. However, neither increasing neither declining trends were statistically significant. In the case of SPI01 the results show positive trends for all sub-regions, but only for S5, S6, and S7 were the trends statistically significant (95% confidence level). Regarding SPEI12, SPEI18, and SPEI24 significant wetting trends were observed for S1, S4, S5, and S6, while drying trends were detected for S2, S3 and S7. For the trends observed in SPEI12 and SPEI18 the drying trend was statistically significant only for region S7, while for the trends observed in SPEI24 the drying trends were statistically significant for regions S2 and S7. In terms of SPI12, SPI18, and SPI24 significant wetting trends were detected for regions S1, S4, S5, S6, and S7, while no significant drying trends were detected for regions S2 and S3. The obtained results indicate that the absolute values of the slope gradually increased when SPEI and SPI were calculated with more lagged months for the S4, S5, S6, and S7 sub-regions (for example, for the S7 sub-region SPEI values were: 0.147×10^{-3} for 1 month, -0.934×10^{-3} for 12 months, -0.1054×10^{-2} for 18 months, and -0.1280×10^{-2} for 24 months). Thus, the drying (wetting) conditions of these sub-regions were more remarkable when SPEI and SPI on the longer timescales were considered. Results from a Mann–Kendall trend test and the Sen slope estimator (not shown) corroborated the regression analysis presented here through a non-parametric approach [83].

Table 2. The slope of the SPEI and SPI at 1, 12, 18, and 24 months timescales for the period 1980–2017. The bold numbers represent positive and negative statistically significant trends at a 95% confidence level. Values in the table are multiplied by 100.

Sub-Regions	SPEI01	SPI01	SPEI12	SPI12	SPEI18	SPI18	SPEI24	SPI24
S1	0.0224	0.0588	0.0810	0.1553	0.0943	0.1826	0.0694	0.1665
S2	-0.0051	0.0141	-0.0276	0.0134	-0.0510	-0.0032	-0.0901	-0.0348
S3	-0.0072	0.0269	-0.0035	0.0463	-0.0195	0.0395	-0.0519	0.0217
S4	0.0132	0.0279	0.0800	0.1167	0.1096	0.1512	0.1413	0.1851
S5	0.0317	0.0712	0.1483	0.2175	0.1850	0.2688	0.2093	0.3089
S6	0.0142	0.0947	0.0916	0.1949	0.1079	0.2297	0.1144	0.2543
S7	0.0147	0.1413	-0.0934	0.15479	-0.1054	0.2067	-0.1280	0.2457

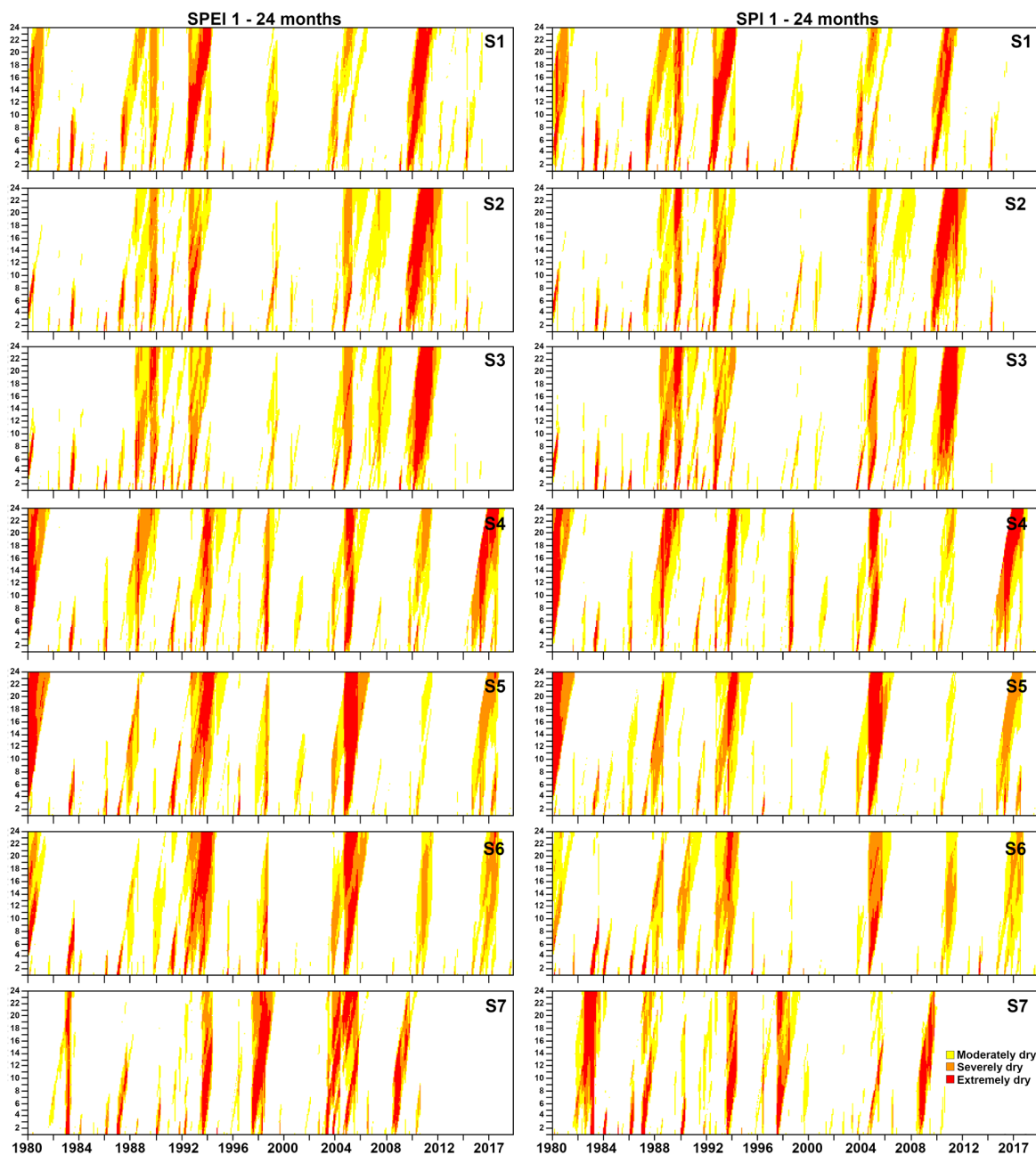


Figure 3. Temporal evolution of the SPEI (left pannel) and SPI (right pannel) from 1- to 24-month timescales for the period 1980–2017 in the S1–S7 climate sub-regions of Vietnam. Yellow, orange, and dark red colors represent moderate, severe, and extreme drought conditions, respectively.

In Table 3 it is observed that differences between the SPEI and SPI trends were negative for all sub-regions and for the timescales of 1, 12, 18, and 24 months. That is, if only the SPI trend was considered, wetter conditions (less dry) than those identified by the SPEI would be obtained due to the omission of the effect of temperature on evapotranspiration processes and the final water balance, which was considered in the formulation of the SPEI. Figure 4 shows the temporal evolution of SPEI12 and SPI12, and their differences as well as the trend lines of each one; it allows a better understanding of the values presented in Table 3. For example, the evolution of the SPEI12 and SPI12 for S5 and S6 showed a positive trend (Figure 4a), but the trend was stronger in the case of SPI12, as shown by the negative trend in the SPEI12–SPI12 index (Figure 4b). Here, we show and further investigate the 12-month timescales of the SPEI and SPI, since trends of both indices at this

scale reflected long-term inter-annual drought changes at the same time considering seasonal extreme events. For 1-, 18-, and 24-month timescales the trends of SPEI and SPI and their difference are available in Figures S1–S3 in the Supplementary Material.

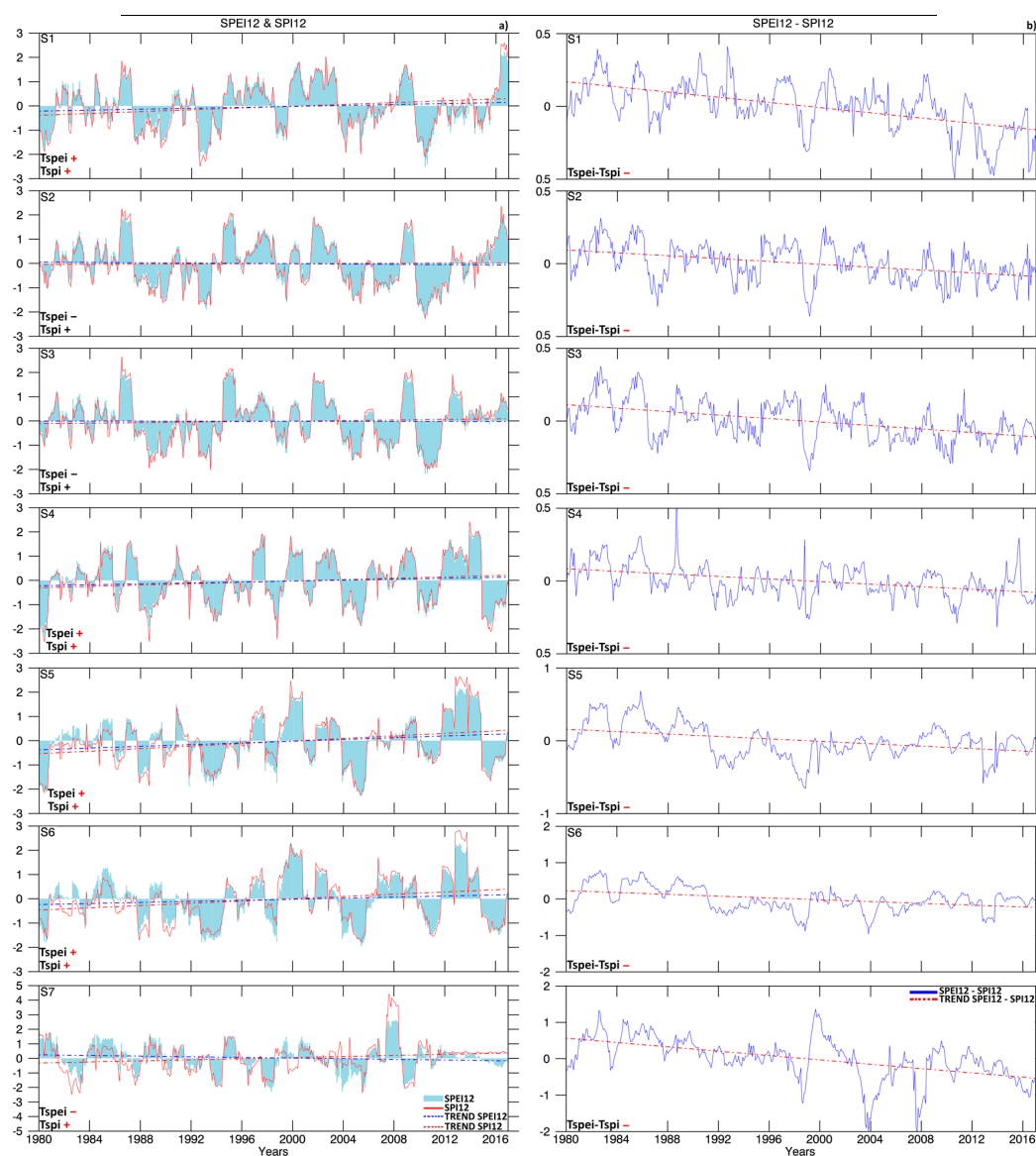


Figure 4. Timeseries of the SPEI12 (shaded in light blue) and SPI12 (red line) (a) and their differences (b) for the seven climate sub-regions of Vietnam during 1980–2017. The dashed blue (red) lines represent the trend of each series. The wetting (drying) significant trends are shown with red +(-) signs at the left bottom of each graphic.

Table 3. The difference between SPEI and SPI at 1-, 12-, 18-, 24-month timescales. All values are statistically significant at a 95% confidence level. Values in the table are multiplied by 100.

Sub-Regions	SPEI01–SPI01	SPEI12–SPI12	SPEI18–SPI18	SPEI24–SPI24
S1	−0.0365	−0.0744	−0.0885	−0.0971
S2	−0.0192	−0.0410	−0.0478	−0.0553
S3	−0.0341	−0.0497	−0.0590	−0.0737
S4	−0.0147	−0.0366	−0.0416	−0.0438
S5	−0.0395	−0.0692	−0.0837	−0.0996
S6	−0.0805	−0.1033	−0.1218	−0.1398
S7	−0.1266	−0.2483	−0.3121	−0.3737

3.3. Drought Episodes

To account for the effects of both the precipitation deficit and changes in temperature, the SPEI was chosen for further analyses at timescales of 1 and 12 months for every climate sub-region, as well as the main indicator to characterize duration and severity. Figure 5a shows the monthly onset frequency of drought episodes for each of the seven climate sub-regions of Vietnam in the period 1980–2017 for SPEI-1. In January, the greatest number of drought episodes began in the northern and central regions, which also occurred for S2 and S3 in February. In March the frequency pattern changed and it was for S5 and S6 that the larger number of drought episodes occurred during this month. A more homogeneous frequency pattern was observed in April, when sub-regions S2 to S5 were affected by a higher number of drought episodes. This condition was very similar for May, when the S6 and S7 remained those regions where fewer drought episodes started. Nevertheless, this changed from June onwards. In June most of the episodes started in the northern (S1, S2, and S3) and southern (S7) regions of Vietnam. Also in July, most of the episodes occurred in the northern and southern regions. In August the greatest number of drought episodes started in regions S4 and S5 and one month later the frequency decreased except for region S6. In September, S6 represents the sub-region in which most of the episodes occurred. However, it is striking that there was a large difference in the frequency of onset of drought episodes between regions S5, S6, and S7, all located in the south of the country. Differences in the annual precipitation cycle can also be seen in the climatology of the precipitation, shown in Figure 2. Nguyen and colleagues [53] argued that S7 region is under the influence of an atmospheric circulation regime that produces an increase in precipitation before the northern regions. In October the onset frequency of drought episodes generally decreased for all sub-regions compared to previous months; the average precipitation of this month preceded the highest accumulated of the rainiest months in the northern regions. However, it was one of the rainiest months in the southern regions. In November the frequency was higher than in October in all regions, and more homogenous from S1 to S4. Finally, in December the onset frequency of drought episodes was higher in S1 and S2 compared to the rest of the sub-regions. In both S1 and S2 the average precipitation for this month was less than the rest of the sub-regions, where it reached the maximum average in the southern S6 and S7 sub-regions. This analysis points to different behaviors between the climate sub-regions in terms of the onset frequency of droughts episodes, and suggests no direct relationship with the climatological average precipitation. This may be due to including flash droughts (episodes with sudden onset and a short duration, e.g., 1 or 2 months) [84], which may be random due to high climatic variability.

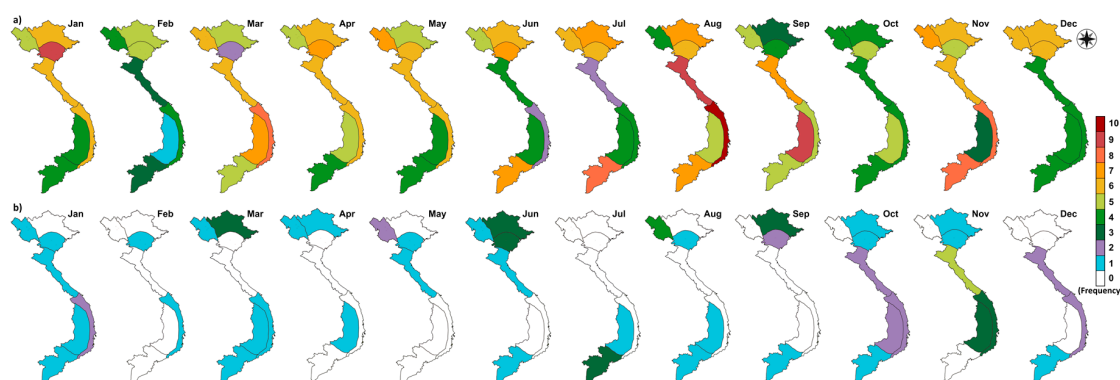


Figure 5. Monthly frequency of drought episode onset in each month for the seven sub-regions of Vietnam, for the period 1980–2017, identified by SPEI01 (a) and SPEI12 (b).

In order to reflect the frequency of the onset for long-term drought episodes, SPEI12 was performed. At this timescale the flash drought episodes were removed, giving more importance for hydrological purposes. As expected, Figure 5b shows an outstanding decrease in frequencies. As with SPEI01, the SPEI12 frequency pattern was very heterogeneous, and no similarities between sub-regions or months can be found. To summarize this information, Figure 6a shows the total number of meteorological and Figure 6b long-term drought episodes that affected each climate sub-region during the period of study. Obviously, due to the higher variability of the SPEI01, it revealed larger numbers of drought episodes. Regions S2, S3, and S5 were affected by more meteorological drought episodes, and S6 the least. SPEI12 showed fewer drought episodes affecting each sub-region, but confirmed that S2 was the most affected and the southern regions the least.

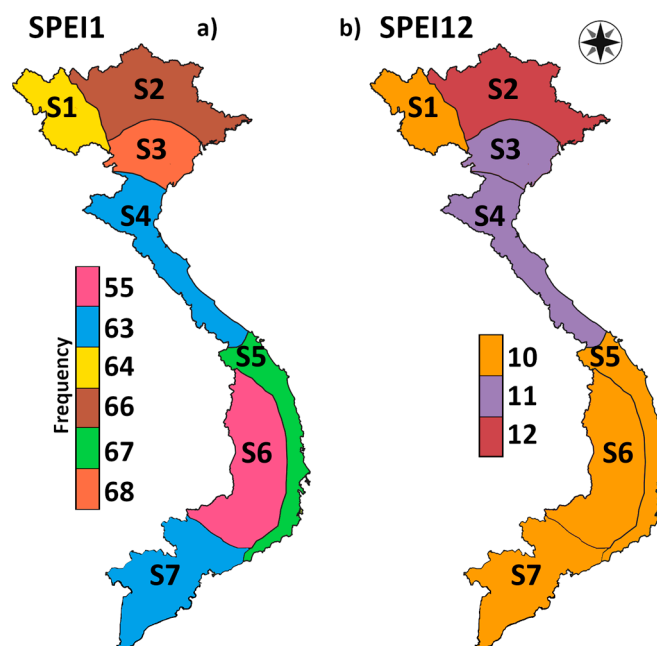


Figure 6. Annual frequency of meteorological and long-term drought episodes for the seven sub-regions of Vietnam during the period 1980–2017 through the SPEI01 (a) and SPEI12 (b), respectively.

The use of other parameters that modulated the impacts of drought episodes as the average duration and severity completed the information of the events. Drought episodes' average duration identified by SPEI01 was generally similar (~2.5 months) for all sub-regions of Vietnam (Figure 7a), revealing the high frequency of flash drought episodes. However, for SPEI12 this did not occur, with S1 and S6 the regions with the longest events (~19 months), while the minimum average duration was in S7 (15 months). In consequence, the average severity of meteorological drought episodes (Figure 7b) was less than that computed for long-term drought episodes.

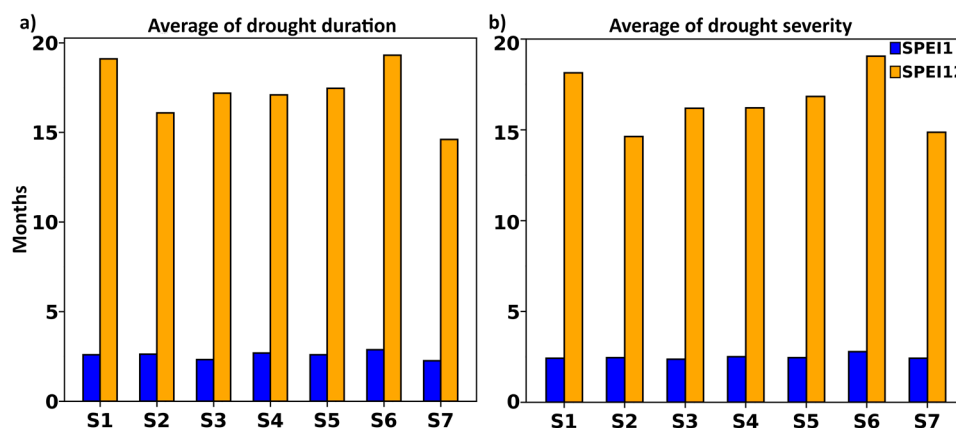


Figure 7. Average of drought duration (a) and drought severity (b) of drought episodes identified through SPEI01 (blue bars) and SPEI12 (orange bars).

3.3.1. Characteristics of the Most Severe Meteorological Drought Episodes

The most severe meteorological drought episodes (assessed by SPEI01) for each sub-region of Vietnam in the period under study according to their severity are shown in Table 4. For S1 and S2 the most severe drought episodes started in July and June (rainy months), respectively, and lasted for nine and seven months, which indicates an impact over subsequent dry seasons. In S3, drought onset was just at the beginning of the rainy season and affected all dry season. In S4 and S5, drought episodes started on the same dates, extending for the following 8 and 10 months, respectively; and finally, in S6 and S7, both episodes began at the same month (December) but in different years and affected several of the following months to conclude with the climatological increase of the precipitation. This is an inherent characteristic of the SPEI01, to reflect most appropriately the water balance conditions of the regions.

Table 4. The most severe meteorological episode for each of the seven sub-regions of Vietnam in the period 1980–2017 and their characteristics.

SPEI01							
Region	Onset	Peak	End	Duration (months)	Severity	Intensity	Peak Value
S1	Jul-2009	Oct-2009	Mar-2010	9	9.02	1.00	−1.99
S2	Jun-2009	Oct-2009	Dec-2009	7	6.31	0.90	−1.36
S3	May-2010	May-2010	Nov-2010	7	6.53	0.93	−1.35
S4	Sep-2004	Oct-2004	Apr-2005	8	7.75	0.96	−1.84
S5	Sep-2004	Oct-2004	Jun-2005	10	9.53	0.95	−2.10
S6	Dec-1990	May-1991	Jul-1991	8	7.40	0.92	−1.68
S7	Dec-1982	Jan-1983	Apr-1983	5	7.83	1.56	−2.20

The development of droughts involves numerous interacting climate processes and various land-atmosphere feedbacks [85]. In particular, the vertical velocity (also represented by omega) has usually been used for drought assessment [86,87]. A vertical cross-section of the mean values and anomalies of omega for the peak month of the most severe drought episodes that affected each climate sub-region between 1980 and 2017 is shown in the top and bottom panels of Figure 8, respectively. Figure 8 represents a vertical latitudinal cross section (from 5° N to 25° N) along the 107° E longitude and from 1000 hPa to 100 hPa. The joint analysis of omega mean values and anomalies allowed a local scale perception of the vertical air displacement (downward, low-level divergence/upward, low-level convergence) over each sub-region associated with severe and extreme drought conditions.

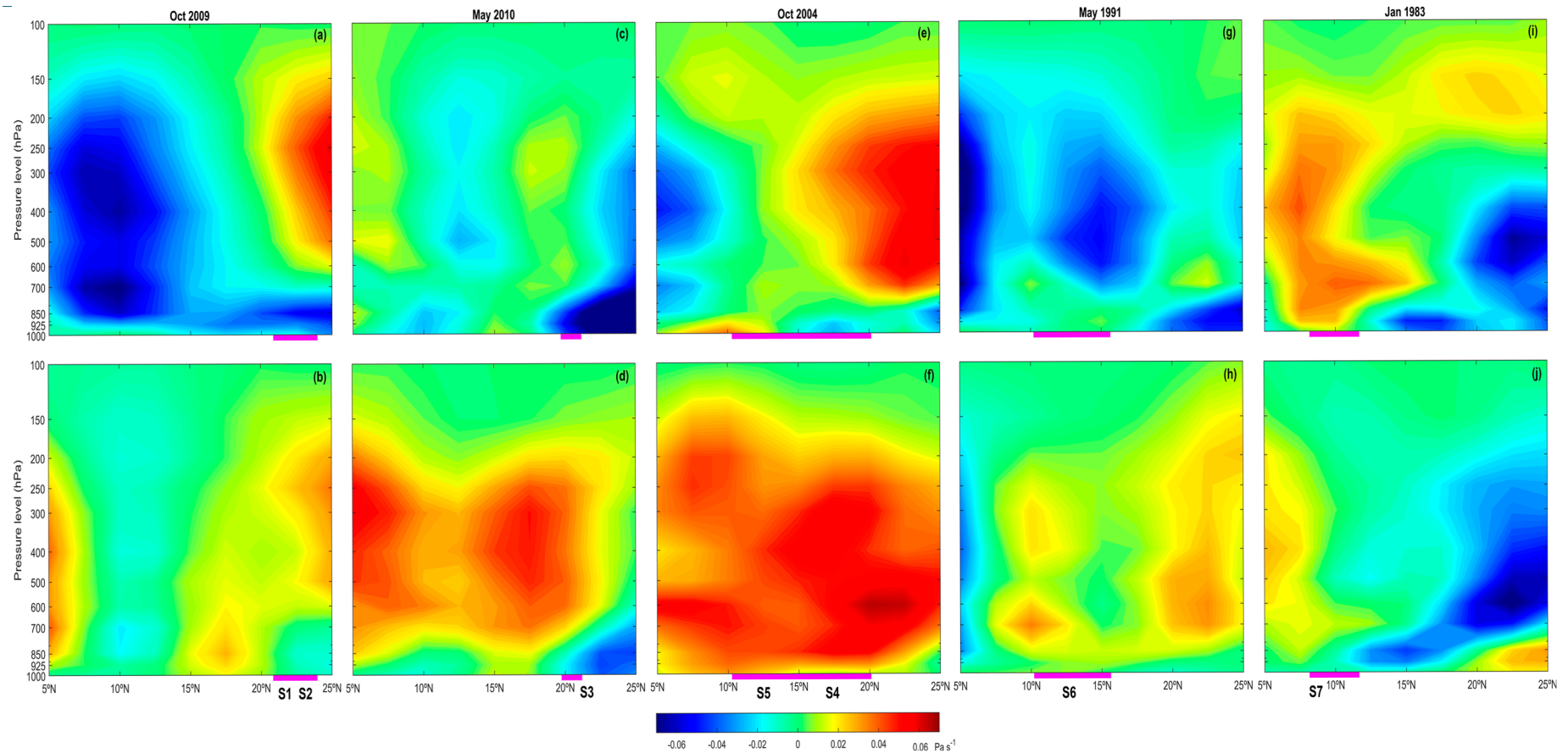


Figure 8. Monthly mean (top panels) and anomalies (bottom panels) of omega (Pa s^{-1}) represented for 107°E and for the peak month of the most severe drought episodes identified 460 (see Table 4) in the period 1980–2017. In the top panels the reddish (bluish) colors represent downward (upward) movements. The pink line represents the approximate latitude of 461 each sub-region. Data from the NCEP-DOE AMIP-II Reanalysis (R-2) [80].

In October 2009 the peaks of the most severe drought episodes in both the S1 and S2 sub-regions occurred simultaneously (Table 4). In this month, negative values of omega were observed in the layer 1000–700 hPa over S1 and S2 (21° N to 23° N, pink line in Figure 8a). On the contrary, above 700 hPa the positive values of omega indicate subsidence and thus forcing divergence at the surface. Positive anomalies of omega on the same layer (Figure 8b) confirmed the enhancement of downward motions that restricted the convergence at the lower troposphere over both S1 and S2. In May 2010, the peak month of the most severe drought episode that affected S3 (Table 4), negative values of omega were observed over S3 (Figure 8c) from 1000 hPa to 700 hPa, which indicate the presence of upward air motions. However, above 700 hPa (4 km), positive values of omega prevail and consequently subsidence and lower troposphere divergence. The vertical cross-section of omega anomalies for this month (Figure 8d) shows that positive anomalies prevailed above 700 hPa, which means that a weakening (strengthening) of upward (downward) motions occurred. For the S4 and S5 sub-regions in Central Vietnam the peak of the most severe drought episode occurred in the same month (October 2004, Table 4). The cross-section of mean values of omega for this month shows positive values under 2 km of height over S5, but negative over S4 (Figure 8e). Above this level mostly positive omega values were observed and therefore subsidence and divergence, as in previous cases. The cross-section of anomalies only shows positive values of this variable, indicating a whole strengthening (weakness) of downward (upward) motions over the region (Figure 8f), suggesting the inhibition of convective motions over the region. For S6, the peak of the most severe episode occurred in May 1991 (Table 4). Omega values over this sub-region in the lowest troposphere were slightly positive and even zero, but they were negative above 850 hPa (Figure 8g). The cross-section of omega anomalies for the same month (Figure 8h) shows that only positive anomalies occurred in the lowest troposphere over S6, which helps to understand the presence of drought conditions. Finally, for the southernmost sub-region (S7), it was observed that omega values were positive along the all vertical column, indicating an environment in which the air mass divergence prevails, and therefore the rainfall inhibition, in agreement with the dry conditions identified. The anomalies of omega for this month also showed mostly positive values over S7. Positive and negative values of omega as well its anomalies in the cross-sections evidence latitudinal climate differences among the sub-regions of Vietnam considered in this study.

These results were confirmed through the patterns shown on the cross-sections of composite anomalies of relative humidity (RH) and air temperature (T) (Figure 9) for the extended period between the drought onset and the peak month of the most severe drought episodes for each one of the seven regions. These patterns exhibited negative RH departures (drier) between −4% and −18% for the total air column over the several sub-regions (Figure 9, upper panels). As previously suggested, there was a strong latitudinal variability, which is particularly evident from the temperature cross-sections. On the one hand, these results show that moisture anomalies are essential during the intensification of these extreme events. On the other hand they suggest that the contribution of temperature positive anomalies is more relevant for the most extreme droughts occurring on the northern regions (Figure 9, lower panels). For the drought event of 2009–2010 affecting the northern regions of Vietnam these results are in agreement with the mechanisms identified for the particularly severe drought in southwestern China during the same period, as described in [88]. Our results also suggest that further research should be performed to better understand the role of moisture and temperature for each of these extreme events and for each sub-region.

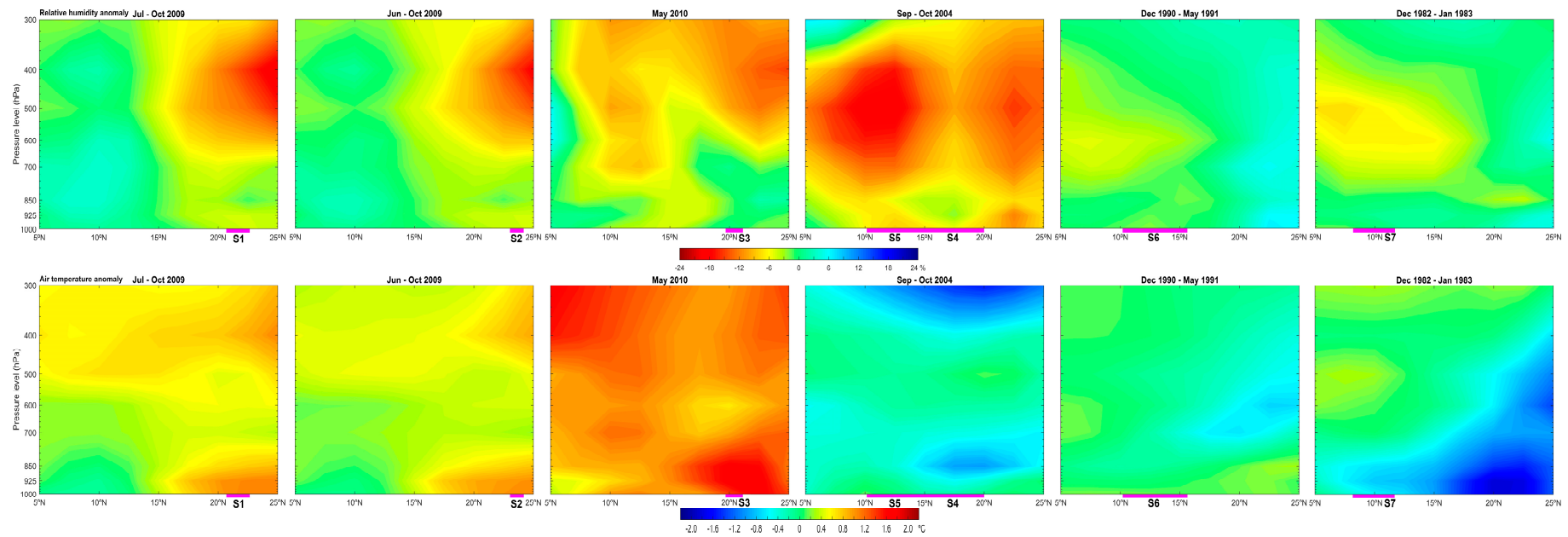


Figure 9. Composite anomalies of relative humidity (in %; **top panels**) and air temperature (in °C; **bottom panels**) represented for 107° E and for the period between onset and peak month of the most severe drought episodes for each of the seven regions of Vietnam according to the SPEI01 series for the period 1980–2017. The pink line represents the approximate latitude of each sub-region. Data from the NCEP-DOE AMIP-II Reanalysis (R-2) [80].

3.3.2. Long-term Drought Episodes

The occurrence and duration of long-term drought episodes assessed through the SPEI considering the accumulation period of 12 months are shown in Figure 10. Drought timescales can be associated with specific drought impacts; at this accumulation timescale the SPEI is usually related to hydrological droughts (e.g., streamflow, reservoir levels). Therefore, agricultural and societal impacts could be expected. As observed, the sequence of episodes shown in Figure 10 illustrates similarity in the onset and length of drought episodes for the S1, S2, and S3 regions. This seemed to change in S4, where the episodes were shorter and had more similar patterns to those that occurred in sub-region S5. In the S6 region the drought episodes also coincided with the onset and duration of most episodes identified in the northern regions. Finally, the greatest temporal difference in the onset and duration of the episodes were for S7, in correspondence with the characteristics of the evolution of drought conditions described in Section 3.2. Despite the hydrological cycle latitudinally varying among the sub-regions, it is well-recognized from this analysis that frequency and duration of long-term dry spells should be largely driven by the climatology of the region.

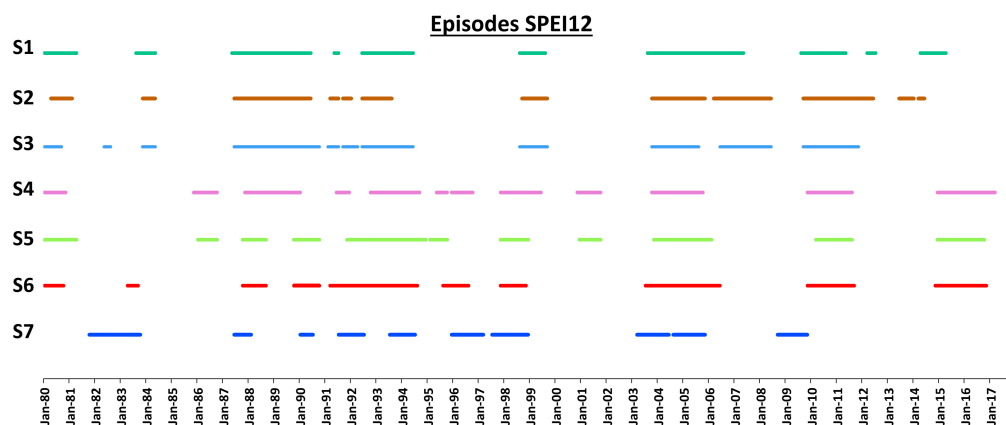


Figure 10. SPEI12 drought episodes which occurred over the seven climate sub-regions of Vietnam during 1980–2017. The episodes were identified following the criteria of Agnew [76].

4. Drought Propagation

Soil moisture represents a key aspect of land-atmosphere interaction and it has an affinity to accumulate atmospheric forcing anomalies, playing an important role in determining the probability of droughts that may affect some regions. For instance, at short timescales (days, weeks) a deficit in precipitation combined with higher evaporation rates leads to a meteorological drought that may propagate into the soil up to the crops. Consequently, it may lead to an agricultural drought and a hydrological drought when both the groundwater and streamflow are affected [12,85,89]. The process can take months and the soil can recall dryness long after the event has occurred. This behavior of memorizing past anomalies is termed soil moisture memory [89,90]. Soil moisture acts as a memory of anomalies in the land surface water budget and, in return, it has a postponed and long-lasting effect on the overlying atmosphere through the land-surface fluxes of heat and moisture [91–93]. Soil moisture contents is linked to plant biomass accumulation in many environments (such as dry, semi-arid, arid) where water availability is the principal regulating factor [94]. It is generally seen as one of the most appropriate variables for monitoring and quantifying the impact of water shortage on vegetated lands due to its influence on the terrestrial biosphere and the feedbacks into the atmospheric system [95,96]. Soil moisture anomaly represents a deviation of current conditions from the usual status of water availability. Therefore, negative anomalies are usually associated with drought conditions. The fact that the soil can remember a wet or dry anomaly is a key aspect of land-atmosphere interactions and has major implications for forecasting [97]. Figure 11 represents the SPEI01 (orange bars) for the most severe drought episode that occurred in S1 and the Soil Moisture root (SMroot) anomaly (blue line).

Knowledge about root-soil moisture memory can enhance climate prediction accuracy, and support agriculture and forest management plans. It can be noted that after the end of the episode (March 2010) the SMroot anomaly continued to be negative during the following six months, meaning that soil reminisces the dry conditions six months after the event has occurred. On the right side of Figure 11 the soil drought memory (SDM) is represented for each of the seven sub-regions of Vietnam after their most severe (MS) drought episode ended. All of them were between two and eight months, with the exception of S6, where SMroot continued to be negative for 28 months.

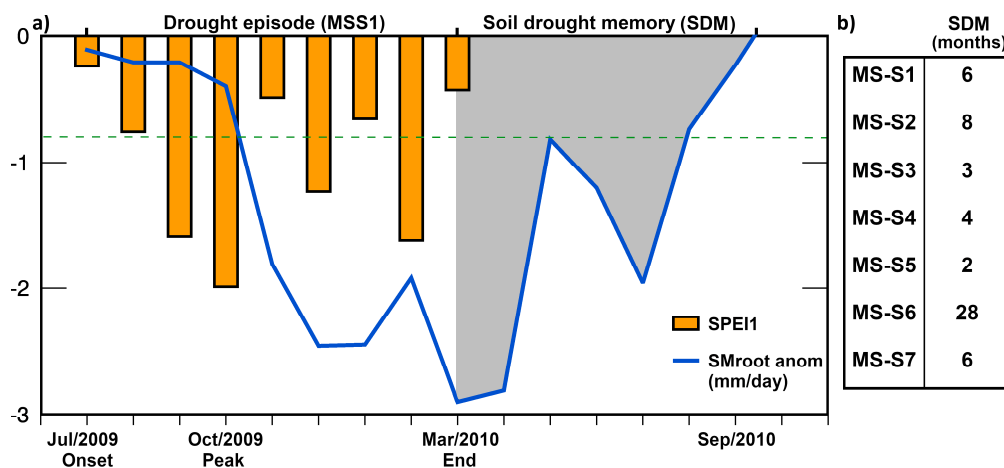


Figure 11. (a) SPEI01 for the most severe drought episode for S1 climate sub-region of Vietnam (MSS1) in the period 1980–2017 (orange bars) and Soil Moisture root (SMroot; mm day^{-1}) anomalies (blue line). (b) Soil drought memory (SDM; months), number of months before the SMroot anomalies became positive after the end of the most severe episode that occurred in each of the seven sub-regions of Vietnam. The discontinuous green line represents the threshold for the identification of a drought episode.

Monthly correlations between the SMroot and the SPEI from 1- to 24-month timescales are shown in Figure 12. In this assessment the maxima r values provided information about the best time scale in which SMroot changes were best associated with dry/wet conditions in each sub-region of Vietnam. For S1, from January to mid-August, the positive correlations indicate that maximum relationships happened with a lag between 2 and 10 months, approximately. After July and August (the rainiest months) the correlation decreased for September and October, but it was still statistically significant until SPEI04. In November and December, the r values increased again for all 24 timescales. As expected, due to its location near S1, the correlation pattern for S2 was very similar to S1. However, according to r values from January to July, the SMroot anomalies were more associated with dry and wet conditions computed considering the last six months. In November and December, the driest months, the correlations were positive for all the SPEI timescales, but major r values were found for the SPEI02 to SPEI06. For the rest of the sub-regions (S4 to S7) the correlations generally decreased. In S4, the values of the correlation highlight that SMroot change during the driest months of the year were strongly related to dry and wet conditions even from last previous months. For S5 and S6 the temporal correlation pattern was very similar but slightly different from the above-described for the northern regions. It is worth noting that in these regions the rainiest months were September, October, and November and maxima correlations between SMroot anomalies and the SPEI occurred from February to July, approximately. This confirms the importance of precipitation amount in the rainiest months on the modulation of dry/wet conditions during climatological driest months. Finally, in the southern sub-region (S7), results show that SMroot in April (the beginning of the rainy season) could be modulated by dry/wet conditions computed in particular from previous dry months (December to March). In the rest of the year, it seems there was a low and no significant relationship. The above-described results indicate that water availability changes in the root zone are largely associated with dry and wet conditions not only from season to season, but also by longer

accumulation periods, and more strongly in the northern regions of Vietnam. These relationships are crucial given that the greatest positive (negative) correlation between SPEI and SMroot also reflects the time scale in which water availability to plants leads to positive (negative) forest response and could be used to perform agricultural plans.

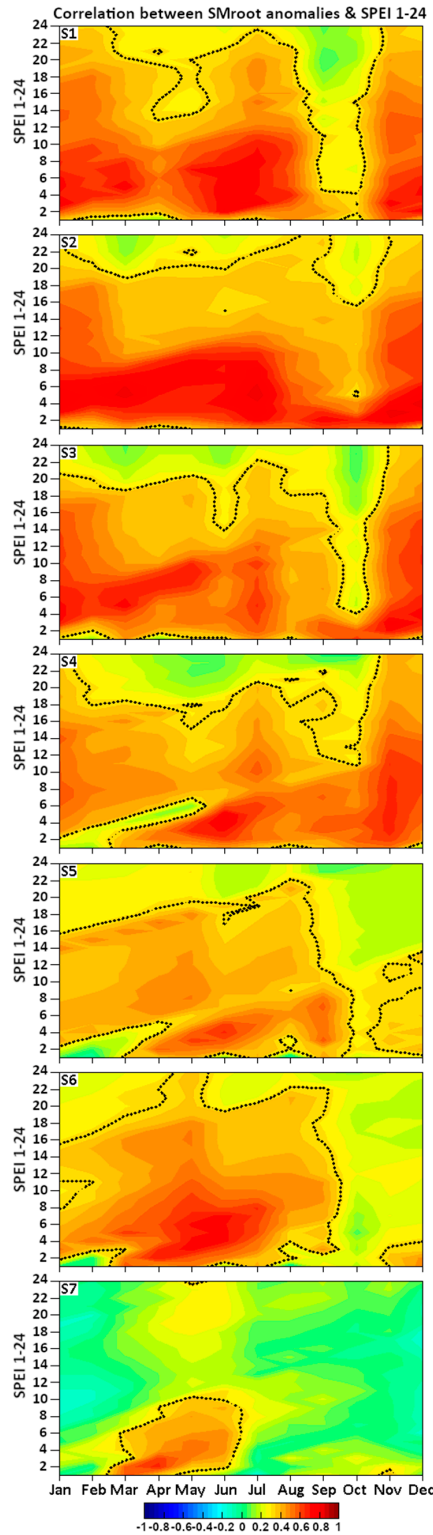


Figure 12. Monthly correlations between Soil Moisture root anomalies (SMroot) and SPEI-01 to SPEI-24 for the seven sub-regions of Vietnam. The dotted lines represent significant correlations at $p < 0.05$.

5. Drought and Teleconnection Patterns Relationship

To investigate the influence of large scale atmospheric and oceanic teleconnection patterns on drought occurrence in the seven climate sub-regions of Vietnam, the Pearson correlation between several indices as BEST, DMI, WHWP, SOI, PDO, and ENSO 3.4 with the SPEI in all the 24 timescales for the period of 1980–2017 were calculated and are shown in Figure 13. For S1, S2, and S3, the best association was found for longer SPEI timescales, and negative correlations during all temporal scales were just found with the SOI (orange line). These results suggest that positive (negative) values of SOI are associated with the occurrence of dry (wet) conditions. The opposite happened with the correlations between the SPEI and the BEST and ENSO 3.4 (principally for S2 and S3), which confirmed that the La Niña phase could be associated with dry conditions in these subregions. No significant correlation was found between PDO, WHWP, and SPEI in S1, but they existed for longer SPEI temporal scales in S2 and S3. The correlations for S4 and southern sub-regions showed some changes compared with the above-described. For S4 a positive relationship (although not statistically significant) between SOI and SPEI (computed for 10 months backward in time) was found. This relationship increased in the southern sub-regions (S5, S6, and S7) for all SPEI temporal scales. Indeed, the positive (negative) correlations of SPEI series with the SOI (BEST, ENSO 3.4) in S6 and S7 were opposite, with the same correlations obtained for S1, S2, and S3, which indicates that the El Niño phase is best associated with dry conditions in southern regions of Vietnam. The El Niño phase is characterized by below-normal air pressure in Tahiti and above-normal air pressure in Darwin, besides abnormally warm ocean waters across the eastern tropical Pacific.

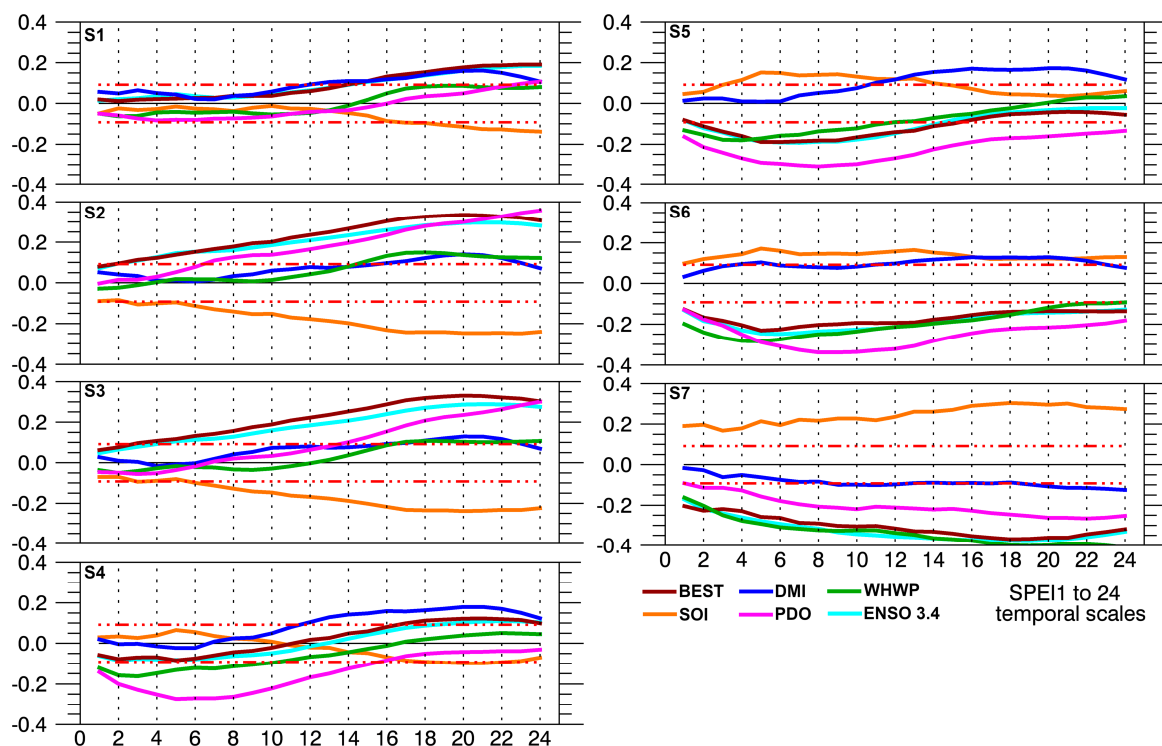


Figure 13. Pearson correlation between the bivariate El Niño Southern Oscillation time series (BEST), Dipole Mode Index (DMI), Western Hemisphere Warm Pool (WHWP), Southern Oscillation Index (SOI), Pacific Decadal Oscillation (PDO), East Central Tropical Pacific SST (ENSO 3.4), and Standardized Precipitation Evapotranspiration Index (SPEI) at the 24-month timescale for the period of 1980–2017. Statistically significant correlation at $p = 0.05$ is indicated by dashed red lines.

Previous findings of Nguyen and co-authors [53] showed that temperature and rainfall variability are shown to be linked to El Niño on both national and sub-regional scales and a most recent study by Le and colleagues [35], using the PDSI and ENSO indices (e.g., MEI (Multivariate ENSO Index), and ONI (Oceanic Niño Index)), confirmed that a positive phase of ENSO (El Niño) is better related to the appearance of dry conditions in southern sub-regions S5, S6, and S7 than the rest in the middle and north of the country. Also, investigating the spatial and temporal variability of SPI over the Indochina Peninsula, Vu and Mishra [98] found a negative correlation between ENSO 3.4 and SPI for the coastal region of Vietnam, indicating that an increase in the Central Pacific SST (El Niño phase) is associated with minor SPI values, and therefore an increase in the probability of droughts. As expected from the increase in correlation for longer timescales of the SPEI with the climate indices, the hydrological droughts would be the best associated with climatic teleconnections. In this sense, Räsänen [99] also found that the hydrological dynamics of the Mekong River have been strongly influenced by El Niño events.

Regarding the correlations obtained with the WHWP and DMI, these results show that a better relationship with the SPEI in all sub-regions exists with the WHWP, being the greatest (and negative) for S7. This indicates that the occurrence of dry/wet conditions in Vietnam, particularly in the south, is best related to the tropical North Atlantic SST increase and extension of the pool rather than anomalous SST gradient between the western equatorial Indian Ocean and the southeastern equatorial Indian Ocean.

The ENSO Influence during Drought Episodes

In this subsection we aim to clarify the different impacts of ENSO on the modulation of dry conditions at each climate sub-region. Figure 14a shows the monthly climatological percentage of Neutral, El Niño, and La Niña conditions during drought episodes identified by the SPEI01 for each of the seven sub-regions of Vietnam. From the northern to the southern sub-regions the percentage of months under El Niño conditions increased latitudinally, reaching 32% of months of drought episodes affected by El Niño in S7. These results were expected from the correlations shown in Figure 12 and from previous studies already referenced. Nevertheless, more than 12% of the months that made up the drought episodes coincided with La Niña conditions. Neutral conditions accounted for more than 50% of the major number of months, which confirms that ENSO is not the only driver of drought in Vietnam.

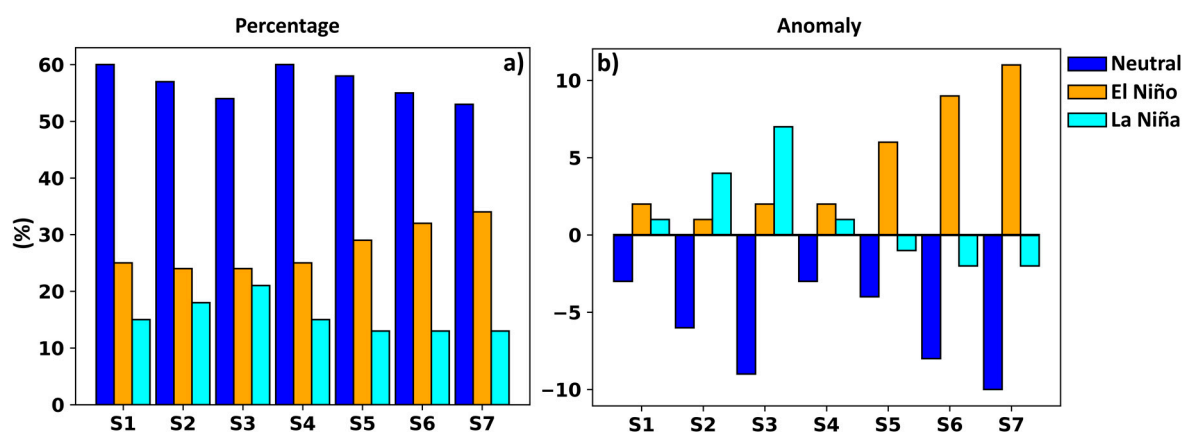


Figure 14. (a) Monthly climatological percentages of Neutral, El Niño, and La Niña conditions during drought episodes identified in SPEI01 for each of the seven sub-regions of Vietnam. (b) The anomalies in the percentage of Neutral, El Niño, and La Niña conditions during all drought months identified in SPEI01 regarding all months in the period of 1980–2017.

Figure 14b shows the monthly climatological percentage departures of Neutral, El Niño, and La Niña conditions presented in Figure 14a from the long-term climatological percentages obtained for all months. Figure 14b confirms that in the S1, S2, S3, and S4 sub-regions the drought episodes were formed by a positive anomaly of the percentage of months during El Niño and La Niña conditions. On the contrary, drought episodes in S5, S6, and S7 were characterized by positive (negative) anomalies on the percentage of months under El Niño (La Niña).

6. Conclusions

In this study, the SPEI and the SPI at timescales from 1 to 24 months were used to investigate the temporal incidence of extreme dry conditions in the seven climate sub-regions of Vietnam during the 1980–2017 period. Results showed that the main periods of drought occurred simultaneously throughout the country in 1992–1993 and 2003–2004, with the exception of 2015–2016, which was not identified for the southern part of the country. In addition, a slight temporary lag could be seen latitudinally (north-south) at the beginning of dry conditions, revealing the difference between the northern and southern sub-regions. A trend analysis revealed the prevalence of a positive trend of both the SPEI and SPI time series corresponding to a tendency to wetter conditions; however, their difference (SPEI–SPI) was always negative, suggesting the importance of temperature and evapotranspiration processes on the intensity of dryer conditions. The absolute value of the trend gradually increased when SPEI and SPI were calculated with more lagged months (longer timescales), showing that the memory of moisture conditions in previous months is accumulated to latter months. To account for the effects of both the precipitation deficit and changes in temperature at different timescales, the SPEI at 1 and 12 timescales was chosen for the detailed identification of the most extreme drought episodes and their respective indicators, such as duration and severity for each climate sub-region. Results revealed that the number of drought episodes did not vary much between regions. However, the average duration and severity of episodes calculated on an annual scale of the SPEI showed differences between regions. In order to see the best timescale with which soil moisture changes were best associated with dry/wet conditions in each climate sub-region, monthly correlation between the soil moisture root anomalies and the SPEI from 1- to 24-month timescales was also provided. Results indicated that the changes in the soil root zone were largely associated with dry and wet conditions not only from season to season, but also by longer accumulation periods and more strongly in the northern sub-regions of Vietnam. Moreover, a study of the most severe meteorological drought episodes also revealed the occurrence of negative anomalies of the root-soil moisture in the subsequent four or more months. Dynamic atmospheric conditions associated with the peak of the most severe drought episodes for every sub-region showed the crucial role of subsidence (and associated inhibition of convective motions) in the middle and high atmosphere. Finally, the linkages between drought conditions in Vietnam and large-scale atmospheric and oceanic teleconnection patterns were different between sub-regions. The obtained results revealed the influence of SOI on wetter and BEST, ENSO 3.4, WHWP, and PDO on drier conditions in southern regions of the country, while the opposite patterns could be observed for some of the northern regions in some timescales. Also, the assessment of the different impacts of ENSO on the modulation of dry conditions in each climate sub-region revealed that from the northern to the southern sub-regions the percentage of months under El Niño conditions increased latitudinally, reaching 32% of months of drought episodes affected by El Niño in S7. These results are in agreement with the findings of Nguyen [49], who found that the effects of El Niño in the southern part are often stronger than in the northern part of Vietnam. Results also showed that more than 12% of the months that made up the drought episodes coincided with La Niña conditions, while neutral conditions accounted for more than 50% of the number of months.

Finally, it is worth stressing that this study allows a better understanding of the relationships between SPI and SPEI in different timescales (1 to 24 months) for each of the seven sub-regions of Vietnam, identifying their trends and variability among regions, as well as the large-scale dynamic atmospheric conditions associated with the characterization of the most severe drought episodes.

Therefore, since today there are freely available large, high resolution datasets and forecasts, better and more efficient monitoring and forecasting of meteorological and hydrological droughts may be now performed. These may contribute to providing early warnings and developing risk management tools tailored to each of these areas where water resources and agricultural production are vital for local economy and populations.

Supplementary Materials: The following are available online at <http://www.mdpi.com/2073-4441/12/3/813/s1>, Figure S1: Time series of the SPEI01 (shaded in light blue) and SPI01 (red line) (a) and their difference (b) for the seven climate sub-regions of Vietnam during 1980–2017. The discontinued blue (red) lines represent the trend of each series. The wetting (drying) significant trends are shown in red +(-) signs at the left bottom of each graphic; Figure S2: The same but for SPEI18; Figure S3: The same but for SPEI24.

Author Contributions: M.S., R.S., M.V. processed the data and wrote the manuscript. M.L.R.L. conceived the idea of the study, processed the data, analyzed the results and revised the manuscript. R.N., L.G. analyzed the results and revised the manuscript. T.P.-V., P.N.B.N., H.D., T.H.C. revised the manuscript. All authors have read and agreed to the published version of the manuscript.

Funding: Fundação para a Ciência e a Tecnologia (UIDB/50019/2020–IDL); Fundação para a Ciência e a Tecnologia and Portugal Horizon2020 (PTDC/CTA-MET/29233/2017); Xunta de Galicia: ED481B 2019/070; Xunta de Galicia: ED481B 2018/062; Xunta de Galicia: Project ED431C 2017/64-GRC; Ministerio de Ciencia, Innovación y Universidades: RTI2018-095772-B-I00

Acknowledgments: M.L.R.L. acknowledges the academic mobility to Vietnam in 2019 under the European Commission Erasmus+ Programme MERGING VOICES 2017-2019 project (KA107-035465/MV18AC0315) and also the academic mobility to the Environmental Physics Laboratory (EPhysLab), Universidade de Vigo, Spain under Fundación Carolina (C.2019). Finally the authors would like to thank two anonymous reviewers and the editor for their thoughtful comments and efforts towards improving the manuscript.

Conflicts of Interest: The authors declare no conflict of interest.

References

- Mishra, A.K.; Singh, V.P. A review of drought concepts. *J. Hydrol.* **2010**, *391*, 202–216. [[CrossRef](#)]
- Dai, A. Drought under global warming: A review. *WIREs Clim. Chang.* **2010**, *2*, 45–65. [[CrossRef](#)]
- Trenberth, K.E.; Dai, A.; Van Der Schrier, G.; Jones, P.D.; Barichivich, J.; Briffa, K.R.; Sheffield, J. Global warming and changes in drought. *Nat. Clim. Chang.* **2014**, *4*, 17–22. [[CrossRef](#)]
- Heim, R.R. A Review of Twentieth-Century Drought Indices Used in the United States. *Bull. Am. Meteor. Soc.* **2002**, *83*, 1149–1165. [[CrossRef](#)]
- Wilhite, D.A.; Sivakumar, M.V.K.; Pulwarty, R. Managing drought risk in a changing climate: The role of national drought policy. *Weather Clim. Extrem.* **2014**, *3*, 4–13. [[CrossRef](#)]
- Otkin, J.A.; Svodoba, M.; Hunt, E.D.; Ford, T.W.; Anderson, M.C.; Hain, C.; Basara, B. Flash Droughts: A Review and Assessment of the Challenges Imposed by Rapid-Onset Droughts in the United States. *Bull. Am. Meteor. Soc.* **2017**, 911–919. [[CrossRef](#)]
- Naumann, G.; Alfieri, L.; Wyser, K.; Mentaschi, L.; Betts, R.A.; Carrao, H.; Spinoni, J.; Vogt, J.; Feyen, L. Global changes in drought conditions under different levels of warming. *Geophys. Res. Lett.* **2018**, *45*. [[CrossRef](#)]
- Lloyd-Hughes, B. The impracticality of a universal drought definition. *Theor. Appl. Climatol.* **2013**, *117*, 607–611. [[CrossRef](#)]
- Leelaruban, N.; Padmanabhan, G. Drought Occurrences and Their Characteristics across Selected Spatial Scales in the Contiguous United States. *Geosciences* **2017**, *7*, 59. [[CrossRef](#)]
- Wang, R.; Peng, W.; Liu, X.; Wu, W.; Chen, X.; Zhang, S. Responses of Water Level in China's Largest Freshwater Lake to the Meteorological Drought Index (SPEI) in the Past Five Decades. *Water* **2018**, *10*, 137. [[CrossRef](#)]
- Tallaksen, L.M.; Van Lanen, H.A.J. Hydrological drought: Processes and estimation methods for streamflow and groundwater. In *Developments in Water Science*; Elsevier Science, B.V.: Amsterdam, The Netherlands, 2004; Volume 48.
- Ionita, M.; Tallaksen, L.M.; Kingston, D.G.; Stagge, J.H.; Laaha, G.; Van Lanen, H.A.J.; Scholz, P.; Chelcea, S.M.; Haslinger, K. The European 2015 drought from a climatological perspective. *Hydrol. Earth Syst. Sci.* **2017**, *21*, 1397–1419. [[CrossRef](#)]

13. Ebi, K.L.; Bowen, K. Extreme events as sources of health vulnerability: Drought as an example. *Weather Clim. Extrem.* **2015**, *11*, 95–102. [[CrossRef](#)]
14. World Meteorological Organization. Drought Monitoring and Early Warning: Concepts, Progress and Future Challenges. 2006. Available online: <http://www.wamis.org/agm/pubs/brochures/WMO1006e.pdf> (accessed on 20 November 2019).
15. Keyantash, J.; Dracup, J.A. The quantification of drought: An evaluation of drought indices. *Bull. Am. Meteorol. Soc.* **2002**, *83*, 1167–1180. [[CrossRef](#)]
16. Vicente-Serrano, S.M.; Van der Schrier, G.; Beguería, S.; Azorin-Molina, C.; Lopez-Moreno, J.I. Contribution of precipitation and reference evapotranspiration to drought indices under different climates. *J. Hydrol.* **2015**, *426*, 42–54. [[CrossRef](#)]
17. Hanel, M.; Rakovec, O.; Markonis, Y.; Máca, P.; Samaniego, L.; Kysely, J.; Kumar, R. Revisiting the recent European droughts from a long-term perspective. *Sci. Rep.* **2018**, *8*, 9499. [[CrossRef](#)]
18. Spinoni, J.; Naumann, G.; Vogt, J.; Barbosa, P. Meteorological Droughts in Europe: Events and Impacts: Past Trends and Future Projections. 2016. Available online: http://www.droughtmanagement.info/literature/EC-JRC_Report%20on%20Droughts%20in%20Europe_2016.pdf (accessed on 20 November 2019).
19. Liberato, M.L.R. Exceptionally extreme drought in Madeira Archipelago in 2012: Vegetation impacts and driving conditions. *Agric. For. Meteorol.* **2017**, *232*, 195–209. [[CrossRef](#)]
20. Wang, Z.; Li, J.; Lai, C.; Zeng, Z.; Zhong, R.; Chen, X.; Zhou, X.; Wang, M. Does drought in China show a significant decreasing trend from 1961 to 2009? *Sci. Total Environ.* **2017**, *579*, 314–324. [[CrossRef](#)]
21. Hoerling, M.; Eischeid, J.; Perlwitz, J.; Quan, X.; Zhang, T.; Pegion, P. On the increased frequency of Mediterranean drought. *J. Clim.* **2012**, *25*, 2146–2161. [[CrossRef](#)]
22. Vicente-Serrano, S.M.; Lopez-Moreno, J.I.; Beguería, S.; Lorenzo-Lacruz, J.; Sanchez-Lorenzo, A.; García-Ruiz, J.M.; Azorin-Molina, C.; Morán-Tejeda, E.; Revuelto, J.; Trigo, R.; et al. Evidence of increasing drought severity caused by temperature rise in southern Europe. *Environ. Res. Lett.* **2014**, *9*, 044001. [[CrossRef](#)]
23. Naumann, G.; Spinoni, J.; Vogt, J.V.; Barbosa, P. Assessment of drought damages and their uncertainties in Europe. *Environ. Res. Lett.* **2015**, *10*, 124013. [[CrossRef](#)]
24. Spinoni, J.; Antofie, T.; Barbosa, P.; Bihari, Z.; Lakatos, M.; Szalai, S.; Szentimrey, T.; Vogt, J. An overview of drought events in the Carpathian Region in 1961–2010. *Adv. Sci. Res.* **2013**, *10*, 21–32. [[CrossRef](#)]
25. Forzieri, G.; Feyen, L.; Rojas, R.; Flörke, M.; Wimmer, F.; Bianchi, A. Ensemble projections of future streamflow droughts in Europe. *Hydrol. Earth Syst. Sci.* **2014**, *18*, 85–108. [[CrossRef](#)]
26. Gudmundsson, L.; Seneviratne, S.I. European drought trends. *Hydrol. Sci.* **2015**, *369*, 75–79. [[CrossRef](#)]
27. Sheffield, J.; Wood, E.F.; Roderick, M.L. Little change in global drought over the past 60 years. *Nature* **2012**, *491*, 435–438. [[CrossRef](#)] [[PubMed](#)]
28. Masih, I.; Maskey, S.; Mussá, F.; Trambauer, P. A review of droughts on the African continent: A geospatial and long-term perspective. *Hydrol. Earth Syst. Sci.* **2014**, *18*, 3635–3649. [[CrossRef](#)]
29. Nguyen, P.L.; Nguyen, M.D. Drought Adaptation and Coping Strategies among Coffee Farmers in the Central Highlands of Vietnam. *J. Agric. Environ. Sci.* **2018**, *8*, 52–66. [[CrossRef](#)]
30. Qian, W.H.; Shan, X.L.; Zhu, Y.F. Ranking regional drought events in China for 1960–2009. *Adv. Atmos. Sci.* **2011**, *28*, 310–321. [[CrossRef](#)]
31. Yu, M.; Li, Q.; Hayes, M.J.; Svoboda, M.D.; Heim, R.R. Are droughts becoming more frequent or severe in China based on the Standardized Precipitation Evapotranspiration Index: 1951–2010? *Int. J. Climatol.* **2013**, *34*, 545–558. [[CrossRef](#)]
32. Tue, M.V.; Raghavan, S.V.; Pham, D.M.; Liong, S.Y. Investigating drought over the Central Highland, Vietnam, using regional climate models. *J. Hydrol.* **2015**, *526*, 265–273. [[CrossRef](#)]
33. Vu, M.T.; Raghavan, V.S.; Liong, S.Y. Ensemble climate projection for hydrometeorological drought over a river basin in central highland. Vietnam. *KSCE J. Civil Eng.* **2015**, *19*, 427–433. [[CrossRef](#)]
34. Ho, C. The Climate Change in Vietnam and Its Impact on Agricultural Sector in Vietnam. Conference in SESAM, UPLB, Philippines. 2018. Available online: https://www.researchgate.net/publication/329024730_THE_CLIMATE_CHANGE_IN_VIETNAM_AND_ITS_IMPACT_ON_AGRICULTURAL_SECTOR_IN_VIETNAM (accessed on 20 November 2019).
35. Le, P.V.V.; Phan-Van, T.; Mai, K.V.; Tran, D.Q. Space-time variability of drought over Vietnam. *Int. J. Climatol.* **2019**, 1–15. [[CrossRef](#)]

36. Intergovernmental Panel on Climate Change (IPCC). *Climate Change 2013: The Physical Science Basis; Contribution of Working Group I to the Fifth Assessment Report of the Intergovernmental Panel on Climate Change*; Intergovernmental Panel on Climate Change: Cambridge, UK; New York, NY, USA, 2013.
37. Intergovernmental Panel on Climate Change (IPCC). *Climate Change 2014: Synthesis Report; Contribution of Working Groups I, II and III to the Fifth Assessment Report of the Intergovernmental Panel on Climate Change*; Pachauri, R.K., Meyer, L.A., Eds.; IPCC: Geneva, Switzerland, 2014; 151p.
38. Nicholls, R.J.; Wong, P.P.; Burkett, V.R.; Codignotto, J.O.; Hay, J.; McLean, R.; Ragoonaden, S.; Woodroffe, C.D.; Abuodha, P.A.O.; Arblaster, J.; et al. Coastal systems and low-lying areas. In *Climate Change 2007: Impacts, Adaptation and Vulnerability. Contribution of Working Group II to the Fourth Assessment Report of the Intergovernmental Panel on Climate Change*; Parry, M.L., Canziani, O.F., Palutikof, J.P., van der Linden, P.J., Hanson, C.E., Eds.; Cambridge University Press: Cambridge, UK, 2007; pp. 315–356.
39. Vien, T.D. Climate change and its impact on agriculture in Vietnam. *J. ISSAAS* **2011**, *17*, 17–21.
40. Dasgupta, S.; Laplante, B.; Meisner, C.; Wheeler, D.; Yan, J. The Impact of Sea Level Rise on Developing Countries. A Comparative Analysis. World Bank Policy Research Working Paper 4136. February 2007. Available online: <https://openknowledge.worldbank.org/bitstream/handle/10986/7174/wps4136.pdf?sequence=1&isAllowed=y> (accessed on 20 November 2019).
41. Raghavan, S.V.; Vu, M.T.; Liong, S.Y. Regional climate simulations over Vietnam using the WRF model. *Theor. Appl. Climatol.* **2016**, *126*, 161–182. [[CrossRef](#)]
42. Thuck, T. Study on Droughts in the South Central and the Central Highlands. *VNU J. Sci. Earth Sci.* **2012**, *28*, 125–132.
43. Nguyen, L.B.; Li, Q.F.; Ngoc, T.A.; Hiramatsu, K. Drought Assessment in Cai River Basin, Vietnam: A Comparison with Regard to SPI, SPEI, SSI, and SIDI. *J. Fac. Agr. Kyushu Univ.* **2015**, *60*, 417–425.
44. Tri, D.Q.; Dat, T.T.; Truong, D.D. Application of Meteorological and Hydrological Drought Indices to Establish Drought Classification Maps of the Ba River Basin in Vietnam. *Hydrology* **2019**, *6*, 49. [[CrossRef](#)]
45. Vu-Thanh, H.; Ngo-Duc, T.; Phan-Van, T. Evolution of meteorological drought characteristics in Vietnam during the 1961–2007. *Theor. Appl. Climatol.* **2014**, *118*, 367–375. [[CrossRef](#)]
46. Nguyen, V.H.; Li, Q.F.; Nguyen, L.B. Drought forecasting using ANFIS—a case study in drought prone area of Vietnam. *Paddy Water Environ.* **2017**, *15*, 605–616. [[CrossRef](#)]
47. Nguyen, L.B.; Le, M. Application of Artificial Neural Network and Climate Indices to Drought Forecasting in South-Central Vietnam. *Pol. J. Environ. Stud.* **2020**, *29*, 1293–1303. [[CrossRef](#)]
48. Hung Le, M.; Perez, G.C.; Solomatine, D.; Medina, V. Studying the impact of infilling techniques on drought estimation—A case study in the South Central Region of Vietnam. In Proceedings of the 2017 Seventh International Conference on Information Science and Technology (ICIST), Da Nang, Vietnam, 16–19 April 2017; p. 292. [[CrossRef](#)]
49. Nguyen, T.D. Coping with Drought in the Central Highlands—Vietnam. Ph.D. Thesis, Institute of Environment and Resources, Technical University of Denmark, 2007. Available online: https://backend.orbit.dtu.dk/ws/portalfiles/portal/127446964/MR2006_147.pdf (accessed on 20 November 2019).
50. Vu, T.M.; Raghavan, S.V.; Liong, S.Y.; Mishra, A.K. Uncertainties of gridded precipitation observations in characterizing spatio-temporal drought and wetness over Vietnam. *Int. J. Climatol.* **2017**, *38*, 2067–2081. [[CrossRef](#)]
51. CGIAR Research Program on Climate Change, Agriculture and Food Security—Southeast Asia (CCAFS SEA). In *Assessment Report: The Drought Crisis in the Central Highlands of Vietnam*; CGIAR Research Program on Climate Change, Agriculture and Food Security (CCAFS): Hanoi, Vietnam, 2016; Available online: <https://ccafs.cgiar.org/publications/drought-crisis-central-highlands-vietnam#.XeQG8ZNKgdU> (accessed on 20 November 2019).
52. FAO UNJP/VIE/037/UNJ 2011. Climate Change Impacts on Agriculture in Vietnam. Available online: <http://www.fao.org/climatechange/34068-0d42acd5f5b7c4d80f3013c038ab92ce6.pdf> (accessed on 20 November 2019).
53. Nguyen, D.; Renwick, J.; McGregor, J. Variations of surface temperature and rainfall in Vietnam from 1971 to 2010. *Int. J. Climatol.* **2014**, *34*, 249–264. [[CrossRef](#)]
54. Sam, T.T.; Khoi, D.N.; Thao, N.T.; Nhi, P.T.; Quan, N.T.; Hoan, N.X.; Nguyen, V.T. Impact of climate change on meteorological, hydrological and agricultural droughts in the Lower Mekong River Basin: A case study of the Srepok Basin, Vietnam. *Water Environ. J.* **2019**, *33*, 547–559. [[CrossRef](#)]

55. Phan, V.T.; Ngo-Duc, T.; Hageman, H.T.M. Seasonal and interannual variations of surface climate elements over Vietnam. *Clim. Res.* **2009**, *40*, 49–60. [[CrossRef](#)]
56. Phan, V.T.; Fink, A.H.; Ngo-Duc, T.; Trinh, T.L.; Pinto, J.G.; van der Linden, R.; Schubert, D. Observed climate variations and change in Vietnam. In *EWATECCOAST: Technologies for Environmental and Water Protection of Coastal Zones in Vietnam, Proceedings of the Contributions to the 4th International Conference for Environment and Natural Resources, ICENR 2014, 17–18 June 2014, Ho-Chi-Minh City, Viet Nam*; Meon, P., Van Phuoc, N., Eds.; Cuveillier: Göttingen, Germany, 2014.
57. Zhang, Y.S.; Li, T.; Wang, B.; Wu, G.X. Onset of the summer monsoon over the Indochina Peninsula: Climatology and interannual variations. *J. Clim.* **2002**, *15*, 3206–3322. [[CrossRef](#)]
58. Ho, T.M.H.; Phan, V.T.; Le, N.Q.; Nguyen, Q.T. Extreme climatic events over Vietnam from observational data and RegCM3 projections. *Clim. Res.* **2011**, *49*, 87–100. [[CrossRef](#)]
59. Linden, R.V.D.; Fink, A.H.; Pinto, J.G.; Phan, V.T. The dynamics of an extreme precipitation event in northeastern Vietnam in 2015 and its predictability in the ECMWF ensemble prediction system. *Weather Forecast.* **2017**, *32*, 1041–1056. [[CrossRef](#)]
60. WMO&GWP. Handbook of Drought Indicators and Indices (M. Svoboda and B.A. Fuchs). Integrated Drought Management Programme (IDMP), Integrated Drought Management Tools and Guidelines Series 2. Geneva. 2016. Available online: http://www.droughtmanagement.info/literature/GWP_Handbook_of_Drought_Indicators_and_Indices_2016.pdf (accessed on 20 November 2019).
61. Palmer, W.C. Meteorological Drought. 1965. Available online: <https://www.ncdc.noaa.gov/temp-andprecip/drought/docs/palmer.pdf> (accessed on 20 November 2019).
62. Wells, N.; Goddard, S.; Hayes, M.J. A self-calibrating Palmer Drought Severity Index. *J. Clim.* **2004**, *17*, 2335–2351. [[CrossRef](#)]
63. McKee, T.B.; Doesken, N.J.; Kleist, J. The relationship of drought frequency and duration to time scales. In Proceedings of the Eighth Conference on Applied Climatology, Anaheim, CA, USA, 17–22 January 1993; pp. 179–184.
64. Vicente-Serrano, S.M.; Begueria, S.; Lopez-Moreno, A.J. A multiscalar drought index sensitive to global warming: The standardized precipitation evapotranspiration index. *J. Clim.* **2010**, *23*, 1696–1718. [[CrossRef](#)]
65. Beguería, S.; Vicente-Serrano, S.M.; Reig, F.; Latorre, B. Standardized Precipitation Evapotranspiration Index (SPEI) revisited: Parameter fitting, evapotranspiration models, tools, datasets and drought monitoring. *Int. J. Climatol.* **2014**, *34*, 3001–3023. [[CrossRef](#)]
66. Allen, R.G.; Pereira, L.S.; Raes, D.; Smith, M. *Crop Evapotranspiration: Guidelines for Computing Crop Water Requirements*. FAO Irrigation and Drainage Paper 56; FAO: Rome, Italy, 1998; 300p.
67. Vicente-Serrano, S.M.; Beguería, S.; Lorenzo-Lacruz, J.; Camarero, J.J.; López-Moreno, J.I.; Azorin-Molina, C.; Revuelto, J.; Morán-Tejada, E.; Sanchez-Lorenzo, A. Performance of Drought Indices for Ecological, Agricultural and Hydrological Applications. *Earth Interact.* **2012**, *16*, 1–27. [[CrossRef](#)]
68. World Meteorological Organization. Standardized Precipitation Index User Guide. 2012. Available online: http://www.wamis.org/agm/pubs/SPI/WMO_1090_EN.pdf (accessed on 20 November 2019).
69. Potop, V.; Boroneant, C.; Možný, M.; Štěpánek, P.; Skalák, P. Observed spatiotemporal characteristics of drought on various time scales over the Czech Republic. *Theor. Appl. Climatol.* **2014**, *115*, 563–581. [[CrossRef](#)]
70. Beniston, M.; Stephenson, D.; Christensen, O.; Ferro, C.; Frei, C.; Goyette, S.; Halsnaes, K.; Holt, T.; Jylhä, K.; Koffi, B.; et al. Future extreme events in European climate: An exploration of regional climate model projections. *Clim. Chang.* **2007**, *81*, 71–95. [[CrossRef](#)]
71. Dai, A. Increasing drought under global warming in observations and models. *Nat. Clim. Chang.* **2013**, *3*, 52–58. [[CrossRef](#)]
72. Potop, V. Evolution of drought severity and its impact on corn in the Republic of Moldova. *Theor. Appl. Climatol.* **2011**, *105*, 1–15. [[CrossRef](#)]
73. Sheffield, J.; Wood, E.F. Projected changes in drought occurrence under future global warming from multimodel, multi-scenario, IPCC AR4 simulations. *Clim. Dynam.* **2008**, *31*, 79–105. [[CrossRef](#)]
74. Liu, Z.; Lu, G.; He, H.; Wu, Z.; He, J. Anomalous Features of Water Vapor Transport during Severe Summer and Early Fall Droughts in Southwest China. *Water* **2017**, *9*, 244. [[CrossRef](#)]
75. Dolado, J.J.; Gonzalo, J.; Mayoral, L. Wald tests of I(1) against I(d) alternatives: Some new properties and an extension to processes with trending components. *Stud. Nonlinear Dyn. Econom.* **2008**, *12*, 1–32. [[CrossRef](#)]

76. Agnew, C. Using the SPI to Identify Drought. In *Drought Network News*; University College London: London, UK, 2000; Volume 12, pp. 6–12. Available online: <https://digitalcommons.unl.edu/droughtnetnews/1> (accessed on 20 November 2019).
77. Harris, I.; Jones, P.D.; Osborn, T.J.; Lister, D.H. Updated high-resolution grids of monthly climatic observations—The CRU TS3.10 Dataset. *Int. J. Climatol.* **2014**, *34*, 623–642. [[CrossRef](#)]
78. Miralles, D.G.; Holmes, T.R.H.; De Jeu, R.A.M.; Gash, J.H.; Meesters, A.G.C.A.; Dolman, A.J. Global land-surface evaporation estimated from satellite-based observations. *Hydrol. Earth Syst. Sci.* **2011**, *15*, 453–469. [[CrossRef](#)]
79. Martens, B.; Miralles, D.G.; Lievens, H.; van der Schalie, R.; de Jeu, R.A.M.; Fernández-Prieto, D.; Beck, H.E.; Dorigo, W.A.; Verhoest, N.E.C. GLEAM v3: Satellite-based land evaporation and root-zone soil moisture. *Geosci. Model Dev.* **2017**, *10*, 1903–1925. [[CrossRef](#)]
80. Kanamitsu, M.; Ebisuzaki, W.; Woollen, J.; Yang, S.K.; Hnilo, J.J.; Fiorino, M.; Potter, G. NCEP-DOE AMIP-II reanalysis (R-2). *Bull. Am. Meteorol. Soc.* **2002**, *83*, 1631–1643. [[CrossRef](#)]
81. Yanai, M.; Li, C.; Song, Z. Seasonal heating of the Tibetan Plateau and its effects on the evolution of the Asian summer monsoon. *J. Meteor. Soc. Jpn.* **1992**, *70*, 319–351. [[CrossRef](#)]
82. FAO. El niño” Event in Vietnam-Agriculture, Food Security and Livelihood Needs Assessment in Response to Drought and Salt Water Intrusion. 2016. Available online: <http://www.fao.org/3/a-i6020e.pdf> (accessed on 20 November 2019).
83. Helsel, D.R.; Hirsch, R.M. Statistical Methods in Water Resources. U.S. Geological Survey Techniques of Water-Resources Investigations. 2002; 510p. Available online: <http://water.usgs.gov/pubs/twri/twri4a3/> (accessed on 20 November 2019).
84. Pendergrass, A.G.; Meehl, G.A.; Pulwarty, R.; Hobbins, M.; Hoell, A.; AghaKouchak, A.; Bonfils, C.J.W.; Gallant, A.J.E.; Hoerling, M.; Hoffmann, D.; et al. Flash droughts present a new challenge for subseasonal-to-seasonal prediction. *Nat. Clim. Chang.* **2020**, *10*, 191–199. [[CrossRef](#)]
85. Wang, W.; Ertsen, M.W.; Svoboda, M.D.; Hafeez, M. Propagation of Drought: From Meteorological Drought to Agricultural and Hydrological Drought. *Adv. Meteorol.* **2016**, 1–5. [[CrossRef](#)]
86. Abatan, A.; Abiodun, B.; Gutowski, W.; Rasaq-Balogun, S. Trends and variability in absolute indices of temperature extremes over Nigeria: Linkage with NAO. *Int. J. Climatol.* **2017**, *38*, 593–612. [[CrossRef](#)]
87. Coelho, C.A.S.; Cavalcanti, I.A.F.; Costa, S.; Freitas, S.R.; Ito, E.R.; Luz, G.; Santos, A.F.; Nobre, C.A.; Marengo, J.A.; Pezza, A.B. Climate diagnostics of three major drought events in the Amazon and illustrations of their seasonal precipitation predictions. *Meteorol. Appl.* **2012**, *19*, 237–255. [[CrossRef](#)]
88. Barriopedro, D.; Gouveia, C.M.; Trigo, R.M.; Wang, L. The 2009/10 drought in China: Possible causes and impacts on vegetation. *J. Hydrometeorol.* **2012**, *13*, 1251–1267. [[CrossRef](#)]
89. Van Lanen, H.A.J. Drought propagation through the hydrological cycle. Climate Variability and Change—Hydrological Impacts. In Proceedings of the Fifth FRIEND World Conference, Havana, Cuba, 27 November–1 December 2006; Volume 308, p. 2006. Available online: <https://pdfs.semanticscholar.org/4b33/54bd536a459fc21442da13ccd2b31ae0e7ee.pdf> (accessed on 20 November 2019).
90. Rahman, M.M.; Lu, M.; Kyi, K.H. Variability of soil moisture memory for wet and dry basins. *J. Hydrol.* **2015**, *523*, 107–118. [[CrossRef](#)]
91. Shinoda, M.; Yamaguchi, Y. Influence of soil moisture anomaly on temperature in the Sahel: A comparison between wet and dry decades. *J. Hydrometeorol.* **2003**, *4*, 437–447. [[CrossRef](#)]
92. Luo, Y.; Berbery, E.H.; Mitchell, K.E.; Netts, A.K. Relationships between land surface and near-surface atmospheric variables in the NCEP North American Regional Reanalysis. *J. Hydrometeorol.* **2007**, *8*, 1184–1203. [[CrossRef](#)]
93. Folwell, S.S.; Harris, P.P.; Taylor, C.M. Large-Scale Surface Responses during European Dry Spells Diagnosed from Land Surface Temperature. *J. Hydrometeorol.* **2016**, *17*, 975–993. [[CrossRef](#)]
94. Schaffer, B.E.; Nordbotten, J.M.; Rodriguez-Iturbe, I. Plant biomass and soil moisture dynamics: Analytical results. *Proc. R. Soc. London A Math. Phys. Eng. Sci.* **2015**, *471*. [[CrossRef](#)]
95. Cammalleri, C.V.; Vogt, J.; Bisselink, B.; de Roo, A. Comparing soil moisture anomalies from multiple independent sources over different regions across the globe. *Hydrol. Earth Syst. Sci.* **2017**, *21*, 6329–6343. [[CrossRef](#)]

96. Green, J.K.; Konings, A.G.; Alemohammad, S.H.; Berry, J.; Entekhabi, D.; Kolassa, J.; Lee, J.E.; Gentine, P. Regionally strong feedback between the atmosphere and terrestrial biosphere. *Nat. Geosci.* **2017**, *10*, 410. [[CrossRef](#)]
97. Seneviratne, S.I.; Koster, R.D.; Guo, Z.; Dirmeyer, P.A.; Kowalczyk, E.; Lawrence, D.; Liu, P.; Lu, C.H.; Mocko, D.; Oleson, K.W.; et al. Soil moisture memory in AGCM simulations: Analysis of Global Land–Atmosphere Coupling Experiment (GLACE) data. *J. Hydrometeorol.* **2006**, *7*, 1090–1112. [[CrossRef](#)]
98. Vu, T.; Mishra, A. Spatial and temporal variability of standardized precipitation index over Indochina peninsula. *Cuadernos de Investigacion Geografica* **2016**, *42*, 221–232. [[CrossRef](#)]
99. Räsänen, T.A. Hydrological Changes in the Mekong River Basin: The Effects of Climate Variability and Hydropower Development. Ph.D. Thesis, Department of Civil and Environmental Engineering, Aalto University, Aalto, Finland, 2014. Available online: <https://aaltodoc.aalto.fi/handle/123456789/13764> (accessed on 20 November 2019).



© 2020 by the authors. Licensee MDPI, Basel, Switzerland. This article is an open access article distributed under the terms and conditions of the Creative Commons Attribution (CC BY) license (<http://creativecommons.org/licenses/by/4.0/>).